FACULTY OF INFORMATION TECHNOLOGY AND ELECTRICAL ENGINEERING
DEGREE PROGRAMME IN ELECTRONICS AND COMMUNICATIONS ENGINEERING

MASTER'S THESIS

Evaluating a Breast Tumor Monitoring Vest with Flexible UWB Antennas and Realistic Phantoms - A Proof-of-Concept Study

Author	Rakshita Dessai
Supervisor	Sami Myllymäki
Supervisor	Mariella Särestöniemi

June 2023

DESSAI R. (2023) Evaluating a Breast Tumor Monitoring Vest with Flexible UWB Antennas and Realistic Phantoms - A Proof-of-Concept Study. University of Oulu, Faculty of Information Technology and Electrical Engineering, Degree Programme in Electronics and Communications Engineering. Master's Thesis, 62 p.

ABSTRACT

This thesis presents a first proof-of-concept for a self-monitoring vest designed for breast cancer detection. The vest operates in the Industrial Scientific and Medical Frequency Band (ISM) 2.5 GHz and ultrawideband (UWB) frequency range of 3.1-10.6 GHz and integrates three types of antennas: UWB monopole with flexible laminate substrate, monopole with conductive textile, and Kapton polyamide-based larger monopole. The performance of these antennas is evaluated to assess their suitability for breast cancer detection. To assess the vest's efficacy, realistic breast tissue-mimicking phantoms and tumor phantoms are developed using novel recipes. These phantoms accurately replicate breast tissue properties and simulate various breast sizes and densities. Tumor detection is achieved through a microwave technique that analyzes channel transfer parameters (S21). Encouraging results demonstrate the vest's capability to detect even small-sized breast tumors (1 cm) across different breast densities, with observed variations in S21 values ranging from 0.5 to 21 dB. This study contributes to the understanding of the influence of antenna design on breast cancer detection by incorporating three distinct antenna types in the self-monitoring vest. The findings validate the vest's potential for early detection of breast tumors, thereby enhancing the possibilities of timely diagnosis and treatment.

Keywords: breast cancer, self-monitoring vest, tissue-mimicking phantoms, dielectric properties, ultrawideband, antennas, microwave technique, tumor detection

TABLE OF CONTENTS

FOREWORD

This master thesis presents a culmination of extensive research on breast tumor monitoring, driven by a shared commitment to advancing healthcare through innovative technologies. It represents a collaborative effort to contribute to a novel solution for accurate and efficient breast tumor detection.

Addressing the global health challenge of breast cancer, the goal was to explore the integration of ultrawideband (UWB) flexible antennas into a monitoring vest, aiming to significantly improve the field and make a meaningful impact.

Throughout this research journey, exciting breakthroughs and complex challenges were encountered. From designing and fabricating realistic tissue phantoms to developing self-monitoring vest with flexible antennas and studying the characteristics of radio channel, every step pushed the boundaries of understanding and propelled the research towards innovative solutions.

I would like to express my sincere gratitude to my supervisors, Sami Myllymäki from the Microelectronics Research Unit, Faculty of Information Technology and Electrical Engineering, and Mariella Särestöniemi from the Health Sciences and Technology research unit, Faculty of Medicine. Their guidance and expertise have been invaluable throughout the research, including their assistance in publishing a research paper on the same topic. Their unwavering support, insightful feedback, and encouragement have shaped the research path and nurtured my growth as researcher. Appreciation is also extended to Microelectronic Research Unit for their generous provision of resources throughout this research endeavor. I also thank my family, friends, and the wider scientific community for their support and contributions.

Reflecting on this research journey, there is a sense of optimism and anticipation for the future. The findings presented in this thesis have the potential to impact the lives of countless individuals, enabling early detection and improved treatment outcomes for breast cancer. It is the sincere hope that this master thesis inspires further research, fosters collaboration, and serves as a steppingstone towards a future where breast tumor monitoring vests become an integral part of breast healthcare, ensuring better health outcomes and enhanced quality of life for individuals worldwide.

Oulu, July, 20 2023

Rakshita Dessai

LIST OF ABBREVIATIONS AND SYMBOLS

AI	Artificial Intelligence
BI-RADS	Breast Imaging Reporting and Data System
CBE	Clinical Breast Examination
CMI	Conditional Mutual Information
CST	Computer Simulation Technology
DAK	Dielectric Assessment Kit
ETRI	Electronics and Telecommunications Research Institute
FEM	Finite Element Method
FP	Fat Phantom
HFSS	High Frequency Structure Simulator
ISM	Industrial Scientific and Medical Frequency Band
LPKF	Leiterplatten-Kopierfräsen
MI	Microwave Imaging
MIS	Microwave Imaging System
MRI	Magnetic Resonance Imaging
MT	Microwave Tomography
NaCl	Sodium Chloride
OSL	Open Short Load
PET	Positron Emission Tomography
PG	Propylene Glycol
SMA	SubMiniature Version A
TEM	Transverse Electromagnetic
TSA	Tapperd Slot Antenna
TRx	Trans receiver
TS	Tumor Sample
TM	Tissue-Mimicking
UWB	Ultra-Wideband
VNA	Vector Network Analyzer
WHO	World Health Organization

1 INTRODUCTION

Breast cancer is a global health concern of paramount importance, affecting millions of women worldwide. In 2020 alone, breast cancer led to over 685,000 deaths, with approximately 2.3 million new cases diagnosed each year [1]. Early detection is critical for improving patient outcomes and treatment success rates. However, existing breast cancer screening methods, such as 3D mammography, breast Magnetic resonance imaging (MRI) with contrast, breast ultrasound, clinical breast examination (CBE), and self-examination, face significant limitations that hinder their widespread adoption outside of hospital settings.

These screening methods encounter several challenges that impact their effectiveness and accessibility. These challenges include cost implications, limited availability of resources, the expertise required for accurate interpretation of results, and patient comfort during screening procedures. Expensive equipment and specialized resources make these screening methods inaccessible in resource-limited settings, while the size and portability of the equipment present practical limitations for home monitoring. Interpreting screening results requires specialized knowledge, and the potential for false positives and false negatives adds complexity to the process. Patient compliance and discomfort during procedures also contribute to low participation rates. Additionally, adherence to recommended screening intervals varies across regions, hindering the full benefits of regular screenings. The World Health Organization (WHO) recommends a 2-year interval for breast cancer screening in women above 50 years of age [1]. However, given the potential aggressiveness and rapid progression of breast cancer, more frequent screenings may be beneficial, particularly for high-risk groups.

1.1 Background and Motivation

To address these limitations, researchers have explored breast cancer monitoring studies based on microwave technology [1]-[8]. The fundamental concept behind this technology is that cancerous tissue exhibits different dielectric properties compared to healthy breast tissue, enabling the detection of cancerous tissue through radio channel responses between multiple antennas placed around the breast. Sensitive receivers capture these differences, and the collected data can be analysed using Artificial Intelligence (AI)-based approaches on server computers.

In a pioneering research paper conducted by the authors in [1], an innovative simulation-based approach was proposed. This approach involved the utilization of UWB flexible antennas embedded in a self-monitoring vest for breast cancer detection. The findings from their research demonstrated the vest's remarkable capability to detect even early-stage small-sized breast tumors (1 cm) located deep within the glandular tissue by analysing channel responses.

1.2 Goal of the Thesis

Building upon this finding, the main objective of this master's thesis is to develop a practical self-monitoring vest equipped with flexible UWB antennas and channel analysis for early detection of small-sized breast tumors. The aim is to address the limitations of current breast cancer screening methods by creating a user-friendly vest that allows regular breast cancer monitoring from home. Through the analysis of radio channel responses, the thesis aims to evaluate the vest's ability to detect 1 cm tumors located deep within the glandular tissue.

Additionally, the research aims to contribute to the advancement of breast cancer detection technology by developing tissue-mimicking phantoms and fabricating flexible antennas in-

house. The thesis includes the design and fabrication of solid samples to create heterogeneous hemispherical breast phantoms representing different breast tissue densities (class II and class IV) [9] and various cup sizes. These samples will be used to test the performance of the self-monitoring vests embedded with three types of flexible antennas. The goal is to improve early detection rates and provide an accessible solution, particularly in resource-limited settings.

1.3 Contribution of the Thesis

The self-monitoring vest is designed to integrate various antenna types, including flexible laminate substrate, textile material, and printed antennas on Kapton material. A novel fabricating technique involving silver ink coating and assistive laser etching is employed for the production of Kapton-based antennas. This approach enables efficient mass production with enhanced control over design and improved reproducibility. The elimination of multiple screens streamlines manufacturing, further advancing the development of the self-monitoring vest.

The antennas integrated into the vest, allow it to operate within the UWB frequency range of 3.1-10.6 GHz, as well as the ISM 2.45 GHz range. The antennas capture radio channel responses from the breast phantom, which are then analysed using channel analysis on a computer. By analysing these responses, the vest can detect even early-stage small-sized breast tumors (1 cm) located deep within the glandular tissue, providing a potentially life-saving advantage for early intervention and treatment.

To ensure accurate evaluation of the self-monitoring vest, realistic 3D breast tissue-mimicking phantoms are developed as an integral part of this master thesis. These phantoms are designed to replicate the complexities of the human breast, including the presence of tumors of various sizes and shapes. The development process involves carefully selecting materials that mimic the dielectric properties of human breast tissue, while also addressing challenges related to ingredient toxicity, accessibility, cost, and stability [10]-[18]. A novel approach is employed, utilizing a non-toxic and durable fat phantom mixture based on pure propylene glycol, which enables precise emulation of breast tissue. This innovative phantom development technique contributes to achieving accurate tissue representation for comprehensive evaluation of the self-monitoring vest.

The evaluation of the self-monitoring vest with flexible antennas and the developed tissue-mimicking phantoms has successfully contributed to the field of wearable technology. Through comprehensive testing and analysis, the dielectric properties of the vest and phantoms were measured and compared to actual breast tissue, providing insights into their performance and fidelity. These findings enhance the overall accuracy and reliability of the breast cancer detection system.

This research aims to improve breast cancer screening by integrating advancements in self-monitoring vest technology, emphasizing the significance of screening intervals, and developing realistic tissue-mimicking phantoms. The derived findings and recommendations provide valuable guidance for the development of more effective and accessible breast cancer screening solutions, with the potential to enhance patient outcomes, reduce mortality rates, and positively impact public health.

1.4 Thesis Outline

The thesis encompasses various sections that collectively contribute to the understanding and exploration of microwave techniques in breast cancer detection. Section 1 provides an introduction, including background, motivation, goal, and contribution. Section 2 presents a

comprehensive background and literature review on topics such as breast anatomy, microwave properties, imaging principles, advantages of microwave techniques, and various microwave approaches for breast cancer detection. Section 3 focuses on the preparation of breast tissue phantoms, covering methodology, ingredient selection, fabrication techniques, and stability assessment. Section 4 discusses the assembly of the final breast phantom for vest evaluation, considering different breast density classes. Section 5 examines the fabricated monitoring vest, including 3 types of flexible antennas and shows different vest versions. Section 6 presents the results of the different vest measurements with breast phantoms created in-house, while Section 7 offers a detailed discussion of the findings. Section 8 provides a summary of the thesis, and Section 9 lists the references used throughout the study.

2 BACKGROUND AND LITERATURE REVIEW

2.1 Anatomy of Female Breast

The female breast can be anatomically divided into two main tissue types: adipose tissue, primarily composed of fat, and fibro glandular tissue, consisting of glands and connective tissue [19]. This anatomical description is depicted in Figure 1.

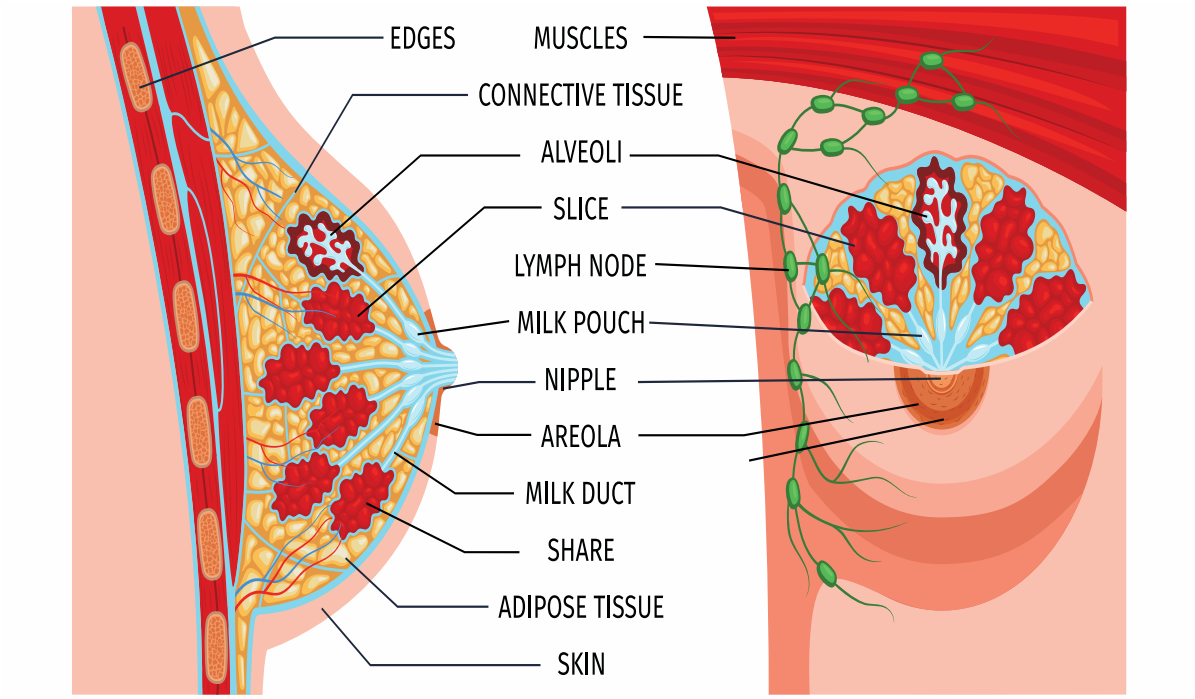

Figure 1. Anatomy of Female Breast

The Breast Imaging Reporting and Data System (BI-RADS) categorizes breasts based on their fibro glandular density, which includes four classes:

1. Class I (Fatty Breasts): These breasts predominantly consist of adipose tissue.
2. Class II (Scattered Fibro glandular Density): Scattered regions of fibro glandular tissue are observed within the breast.
3. Class III (Heterogeneously Dense Breasts): Fibro glandular tissue constitutes a substantial portion of the breast.
4. Class IV (Extremely Dense Breasts): There is minimal adipose tissue present, and the breast is predominantly composed of fibro glandular tissue.

Mammograms illustrating breasts belonging to each of these BI-RADS classes are presented in Figure 2. Breast density plays a significant role in tumor detection, as dense breasts can pose challenges in distinguishing tumors from normal glandular tissue during traditional mammography. Consequently, there is a need for alternative imaging methods that are safe, comfortable, and capable of effectively detecting tumors in denser breast tissue.

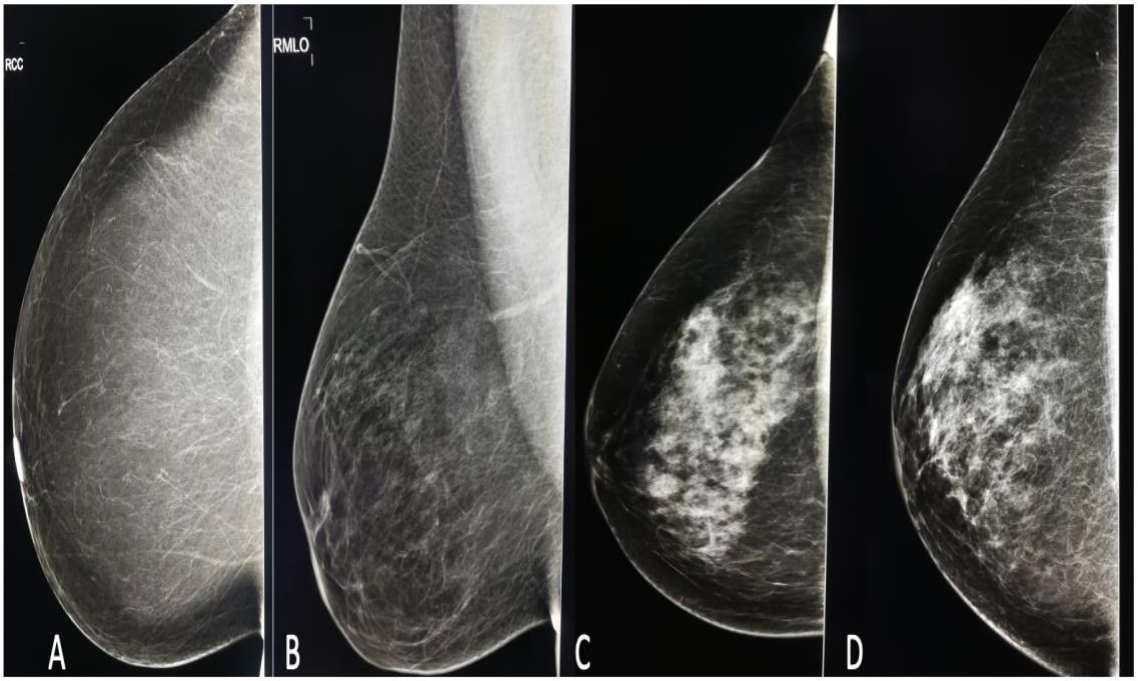

Figure 2. Mammograms depicting (A) fatty, (B) scattered, (C) heterogeneously dense, and (D) extremely dense breasts

2.2 Microwave Properties of Human Breast

Human breast tissue exhibits specific microwave properties that can be characterized by its dielectric properties, including relative permittivity and conductivity. These properties play a crucial role in the interaction of microwave radiation with breast tissue during imaging and detection processes. The electromagnetic properties of breast tissue have been investigated across different frequency ranges, as highlighted in Gabriel et al.'s extensive review [20].

The dielectric properties of human breast tissue depend on several factors, including the composition and structure of the tissue. The relative permittivity of breast tissue varies with the frequency of the applied microwave radiation. At lower frequencies, the relative permittivity is primarily influenced by the water content in the tissue, while at higher frequencies, the contribution of other constituents becomes more significant. The relative permittivity is typically represented by complex values, consisting of a real part (permittivity) and an imaginary part (loss factor). The real part represents the ability of the tissue to store electrical energy, while the imaginary part represents the energy dissipation or absorption within the tissue.

Similarly, the conductivity of breast tissue is an important microwave property that indicates the tissue's ability to conduct electrical current. It is related to the ion concentration and mobility within the tissue. Conductivity is influenced by factors such as water content, electrolyte concentration, and the presence of ions in the tissue.

To assess the dielectric properties of breast tissue, measurement techniques such as microwave spectroscopy or microwave tomography are commonly used. These techniques

involve transmitting and receiving microwave signals through the tissue and analyzing the reflected or transmitted signals to extract information about the tissue's dielectric properties.

The human breast consists of different layers, each with varying electrical properties that influence the behavior of microwave radiation and its penetration into the tissue. The outermost layer of the breast is the skin, which has relatively low water content and exhibits lower relative permittivity and conductivity compared to the underlying breast tissue. The skin acts as a barrier to microwave penetration and can cause partial reflection of the incident waves.

Most of the breast is composed of adipose tissue, which consists mostly of fat cells. Adipose tissue has low relative permittivity and conductivity, primarily due to its low water content. Microwave radiation tends to propagate through adipose tissue with minimal absorption and attenuation.

Another layer in the breast is the fibro glandular tissue, which contains glands, ducts, and connective tissue. This tissue has higher water content compared to adipose tissue, resulting in higher relative permittivity and conductivity. Microwave radiation experiences increased absorption and attenuation when passing through fibro glandular tissue.

The variation in electrical properties across these breast layers influences the behavior of microwave radiation during breast imaging. Microwave signals tend to penetrate deeper into adipose tissue due to its lower absorption and attenuation properties. On the other hand, microwave penetration is limited in fibro glandular tissue due to its higher absorption and attenuation.

The depth of microwave penetration depends on the frequency of the radiation used. Lower frequencies, such as in the range of a few hundred megahertz, can penetrate deeper into the breast, reaching the underlying fibro glandular tissue. Higher frequencies, such as in the range of several gigahertz, have shallower penetration depths, primarily interacting with the superficial layers of the breast.

The detection of abnormalities or anomalies in the breast using microwave imaging techniques relies on the differences in the dielectric properties of healthy tissue and pathological conditions, such as tumors or lesions. By measuring the reflected or transmitted microwave signals and analysing their changes, it is possible to identify and characterize these anomalies.

Various studies have focused on detecting breast tumors by studying female breast tissues. Researchers have conducted experiments on fresh human malignant and normal breast tissues to examine their properties. For instance, Lazebnik et al. performed a comprehensive analysis of the dielectric properties of normal, benign, and malignant breast tissues [21].

In conclusion, understanding the electrical properties of each breast layer and the behavior of microwave radiation within the breast is crucial for designing effective microwave imaging systems, optimizing imaging parameters, and improving the accuracy of breast cancer detection and characterization.

2.3 Basic Principle of Microwave Channel Analysis

The basic principle of microwave channel analysis is based on the propagation of microwaves through the breast tissue and the detection of changes caused by the presence of a tumor. Microwave channel analysis systems rely on antenna sensors to enable the transmission and reception of signals. The transmitting antenna generates and emits microwave signals into the breast tissue. As the microwave signals travel through the breast tissue, they interact with any tumors present. The presence of a tumor causes scattering phenomena, leading to changes in the propagation characteristics of the microwaves as shown in Figure 3. The receiving antenna, positioned on the opposite side of the breast, captures the scattered microwave signals after they

have passed through the tissue. The antenna detects variations in the amplitude, phase, and polarization of the received signals, which carry information about the presence and characteristics of the tumor [22]. The collected microwave signals are processed and analyzed to reconstruct an image of the breast tissue. Advanced algorithms and imaging techniques are employed to extract relevant information about the tumor, such as its location, size, and electrical properties.

Increasing the frequency of microwaves has the potential to improve image resolution, but it also poses challenges in terms of increased tissue loss. This trade-off between resolution and tissue penetration needs to be carefully considered to obtain clear and informative images. Achieving clear and high-resolution microwave images is still an active area of research. There is an upper frequency limit that should be established to ensure sufficient tissue penetration. In cases where tissue penetration is a concern, the use of ultra-wideband signals proves beneficial. For instance, when using a microwave signal centred at 6 GHz, the penetration loss in healthy fat tissue remains below 4 dB/cm [23]. This characteristic enables the transmission of low-power signals to an antenna positioned on the opposite side of an object, facilitating effective imaging.

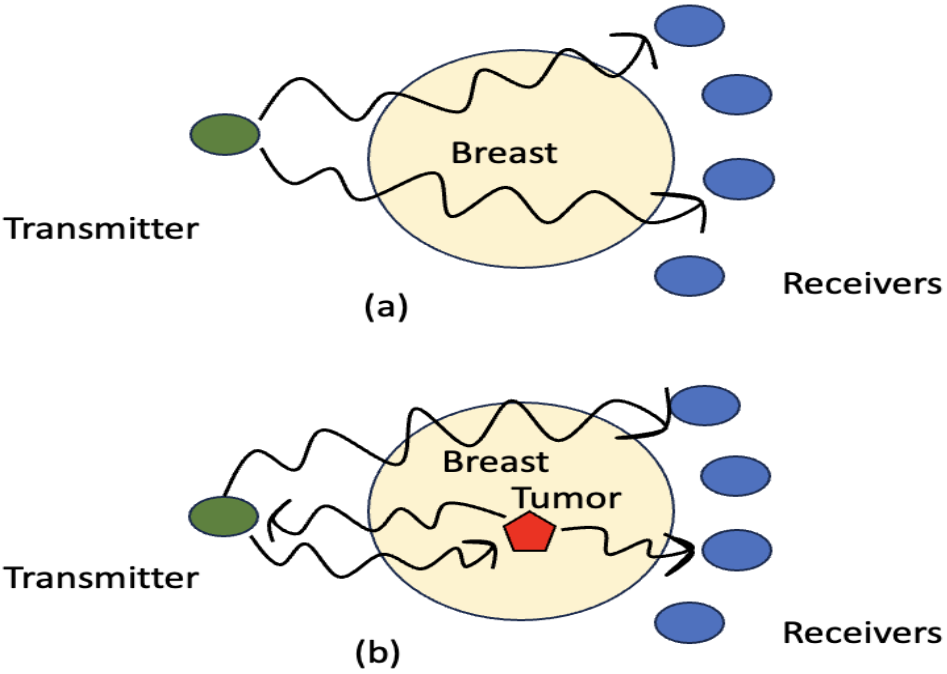

Figure 3. The basic microwave channel analysis problem a) involves illuminating the breast with microwaves and detecting energy traveling through or reflected from the breast b) Presence of tumor, changes the reflected and transmitted waves compared to (a)

2.4 Advantages of Microwave-Based Tumor Detection

Microwave-based tumor detection, with a focus on microwave channel analysis, offers significant advantages in the field of medical imaging. Here are the detailed benefits:

1. Non-Invasive Imaging: Microwave-based tumor detection is a non-invasive technique, eliminating the need for invasive procedures such as biopsies. This ensures patient comfort and reduces the associated risks and complications.
2. Deep Tissue Penetration: Microwaves can penetrate biological tissues deeply due to their longer wavelengths. This allows microwave-based imaging to detect tumors located in hard-to-reach areas within the body, even in regions that may be challenging to access using other imaging modalities.
3. Analysis of Electromagnetic Wave Interaction: Microwave-based tumor detection relies on the interaction between microwave electromagnetic waves and biological tissues. By analyzing this interaction, valuable information about the electrical properties of tumors, such as electrical conductivity and relative permittivity, can be obtained.
4. Contrast Enhancement: Tumors often exhibit distinct electrical properties compared to surrounding healthy tissues. Microwave channel analysis exploits these differences to enhance the contrast between tumors and normal tissues. This enhanced contrast enables more accurate localization and characterization of tumors.
5. Real-Time Imaging: Microwave imaging systems can provide real-time or near real-time imaging capabilities. This real-time monitoring allows for dynamic assessment of tumor behavior and response to treatment, enabling prompt decision-making and adjustment of treatment plans.
6. Integration with Other Imaging Techniques: Microwave-based tumor detection can be integrated with other imaging modalities, such as ultrasound, magnetic resonance imaging (MRI), or X-ray, to combine their complementary strengths. This multi-modal integration enhances the accuracy and reliability of tumor detection, localization, and characterization.
7. Quantitative Analysis: Microwave channel analysis enables quantitative assessment of tumor properties, such as tumor size, shape, and composition. This quantitative information provides clinicians with valuable data for treatment planning and monitoring the effectiveness of therapies.
8. Multi-Frequency Analysis: Microwave-based tumor detection can involve the analysis of multiple frequencies to capture a more comprehensive picture of tumor properties. By analyzing the response of tumors at different frequencies, it is possible to obtain a more detailed understanding of their electrical and structural characteristics.
9. Imaging System Optimization: Microwave channel analysis aids in optimizing the design and configuration of microwave imaging systems. By analyzing the channel characteristics, such as signal strength, noise, and interference, it becomes possible to optimize the system parameters, such as antenna design, frequency selection, and power settings, for improved tumor detection performance.

In summary, the advantages contribute to improved accuracy and reliability in tumor detection, localization, and characterization, ultimately leading to better clinical outcomes in the field of medical imaging.

2.5 Various Microwave Techniques in Breast Cancer Detection

In recent years, microwave-based techniques and UWB antennas have been extensively studied for their potential in breast cancer detection and imaging. These approaches employ various antennas operating within specific frequency bands and utilize imaging methods such as

microwave tomography and UWB radar [1]. Moreover, in the context of breast cancer detection and self-monitoring, there have been advancements in the development of wearable technologies, such as self-monitoring vests, integrated with UWB antennas. These vests are equipped with UWB radar systems that continuously monitor the breast tissue. They can detect changes in tissue properties, such as variations in electrical conductivity or relative permittivity, which could indicate the presence of abnormalities or tumors.

2.5.1 Microwave Tomography

Microwave tomography is a technique used to reconstruct the electrical properties of the breast at each pixel. Meaney et al. has developed a clinical prototype, for active microwave imaging of the breast, demonstrating promising results in tumor detection and breast density analysis. Their system employs a 32-channel data acquisition system and 16 circularly arranged monopole antennas operating in the frequency range of 300 MHz to 1 GHz. Notably, a liquid immersion medium is utilized during the imaging process. Each antenna sequentially transmits an electromagnetic wave which propagates through the breast within the imaging region. Measurements are collected at the remaining 15 antennas so that those close to the radiator mainly measure waves reflected from tissue surfaces whereas those opposite to the transmitter mainly measure transmitted waves depicted in Figure 4. The multi-view scattered intensity and phase distributions reveal the local dielectric properties of transilluminated tissues, enabling the prototype to effectively differentiate tumors larger than 1 cm from benign lesions [24]. In their subsequent research, the Dartmouth group explores the utilization of 3D Finite Element Method (FEM) microwave tomography. This approach, coupled with advancements in hardware and software have resulted in a data acquisition time of less than 2 minutes and image processing within 20 minutes, offering a significant improvement over traditional method [25]-[26].

In Korea, Seong-Ho et al. developed an Electronics and Telecommunications Research Institute microwave tomography (ETRI MT) system, an advanced modification of the system by Meaney et al., operating in the frequency range of 500 MHz to 3 GHz. This high-technology preclinical prototype, equipped with a circular array of 16 transmitting-receiving (TRx) antennas, allows vertical adjustment, and utilizes a high-sensitivity TRx device and a microwave switch matrix with high channel isolation. The system employs software for accurate microwave image reconstruction, resulting in reliable and informative images compared to approximated algorithms like Conditional Mutual Information (CMI). In one experiment, the prototype system successfully detected a 5 mm tumor inside a phantom at a frequency of 1300 MHz [27].

Amineh et al. introduced a near-field microwave imaging system based on UWB antennas, incorporating a raster scan algorithm [28]. The study presented both measured and simulated outcomes using a 3D homogeneous breast phantom and a heterogeneous model. It is important to note that the phantom used in the study does not accurately represent a real breast and lacks a 360° rotation angle for scanning. The proposed system utilized a directive Transverse Electromagnetic (TEM) horn antenna, enhancing the scattering signal from the dielectric phantom. The antennas of the system were in direct contact with the imaging domain.

Each study contributes unique aspects, such as hardware advancements, software improvements, and imaging approaches, highlighting the ongoing efforts to enhance tumor detection and characterization in microwave tomography for breast imaging.

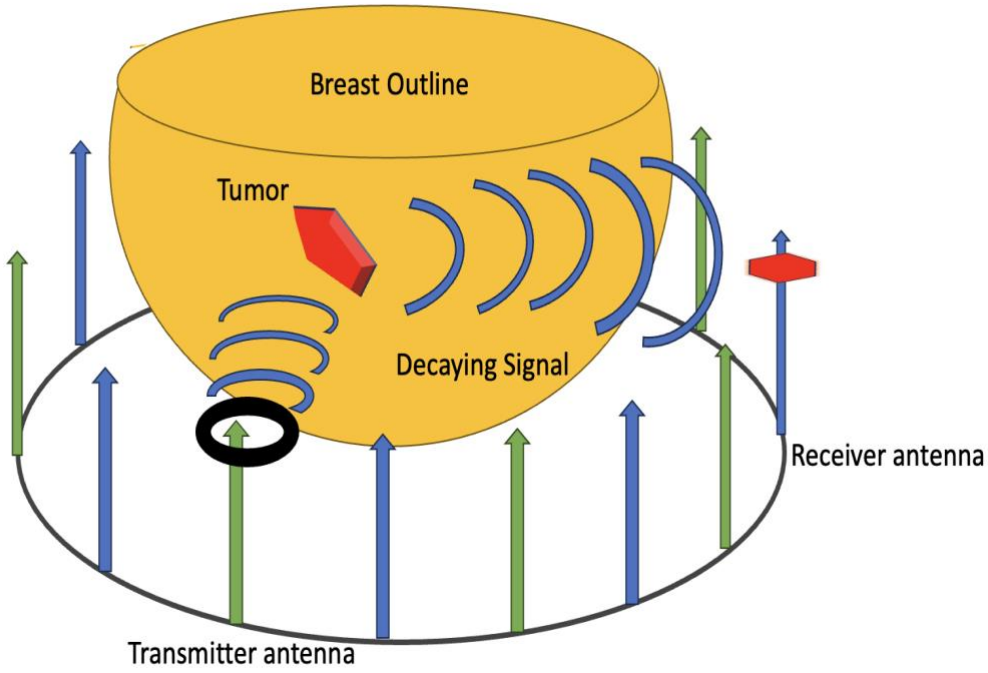

Figure 4. Schematic 3-D representation of tomographic microwave imaging setup

2.5.2 Radar-Based UWB Microwave Imaging

In radar based imaging signal processing techniques were employed to identify regions of strong backscatter similar to conventional radars. The regions of large backscatter indicate the presence of a contrast in electrical properties such as the contrast between cancerous and healthy tissue. Whereas tomographic systems aim to reconstruct an image of the dielectric properties themselves, radar based systems try to map the location of microwave scatterers without determining their specific properties. It is thus a qualitative technique whereas tomography can be considered a quantitative technique.

Flores et al. conducted a preclinical experimental study using a single-element Vivaldi antenna to investigate cylindrical-shaped dielectric objects. The reflection coefficient (S11) was measured in an imaging domain consisting of a plexiglass tank filled with canola oil [29]. To improve the quality and accuracy of the images, a circular scanning geometry and a rotating platform for the phantom were employed.

Mohammed et al. proposed a microwave imaging system utilizing a 12-element Tapperd Slot (TSA) planar antenna configuration. The system was evaluated for breast imaging applications, employing a plastic container filled with canola oil to submerge the water cylinder, conductor, and dielectric. Mutual coupling effects were investigated using a trust region framework [30]. However, the study did not provide specific information on the signal and image processing techniques employed. It mainly focused on analysing mutual coupling rather than comprehensive breast imaging capabilities.

Klemm et al. from the University of Bristol developed an ultra-wideband microwave imaging system operating at higher frequencies (4.5-10 GHz) compared to the system of Meaney et al. This was achieved by utilizing cavity-backed patch antennas instead of monopole

antennas. Additionally, Klemm et al. employed a 3D hemispherical antenna array as opposed to the 2D circular array used by Meaney et al. The system utilizes a multi-static radar-based detection approach with a novel hemispherical real-aperture antenna array consisting of 16 UWB aperture-coupled stacked-patch antennas [31]. It is designed for use with realistic 3D breast phantoms and has been tested during initial clinical trials with real breast cancer patients.

The properties of the antenna play a fundamental role in determining the exact position of the tumor, and because of this, some research groups have been interested in the optimization of antennas used in these systems.

Overall, these diverse approaches contribute to the ongoing advancements in microwave-based breast imaging for tumor detection and characterization.

2.5.3 Different Self-Monitoring Vests with UWB Antennas

While several solutions using MT and UWB Radar have reached the clinical trial stage and achieved promising outcomes, most existing systems are large-scale and primarily designed for hospital use [1]. However, there is a growing interest in developing self-monitoring devices for microwave-based breast cancer detection [8]. These devices aim to provide easily accessible tools that can reach a broader population, including women who may refuse or face challenges in participating in regular screenings. A novel concept introduced involves the integration of wearable, flexible UWB antennas into a self-monitoring vest [8]. This approach enables women to monitor their breast health more frequently, facilitating the timely detection of aggressive cancers that may rapidly progress.

Significant efforts have been made to design and evaluate UWB antennas specifically for breast cancer detection. Flexible UWB antennas, embedded in the self-monitoring vest, have shown promise in providing accurate and non-invasive imaging capabilities [32]-[34]. Operating within the standardized UWB band and the ISM band at 2.4 GHz, these antennas offer versatility and compatibility with existing systems [35]. Their design ensures good impedance matching and adaptability to different breast positions and curvatures [32]-[33]. Furthermore, conformal UWB antenna arrays, resembling a bra, have been developed to improve the penetration of electromagnetic waves into the breast tissue, thereby enhancing imaging performance [8].

Bahrami et al. developed a flexible monopole UWB antenna array for breast cancer microwave imaging in the 2-5 GHz spectrum. By modifying an existing system model, they replaced the bulky and expensive traveling wave tapered and loaded transmission line antenna array with a flexible monopole antenna array [36]. Through 3D simulations using the high frequency structure simulator (HFSS) software, they accurately modelled the antenna propagation in the presence of inhomogeneous breast media. The results demonstrated the suitability of the proposed antenna as part of a synthetic aperture array for breast cancer detection. The researchers designed a compact monopole antenna on a 100 μm Kapton polyimide substrate, optimized for impedance matching. They also developed a flexible conformal 4x4 ultra-wideband antenna array, resembling a bra, as the core of a multi-static imaging system for radar-based breast cancer detection. Similarly, in a study [8] researchers have used 50-μm Kapton polyimide substrate for antenna fabrication.

Rahman et al. developed a compact, ultra-wideband antenna on a flexible substrate for microwave imaging operating in the 4-6 GHz frequency range [37]. The researchers employed a specific compound, 5-(4-(perfluorohexyl) phenyl) thiophene-2-carbaldehyde, to achieve the desired properties. Unlike traditional arrays, they proposed a bi-static radar-based imaging system with two omnidirectional antennas, reducing complexity and size. The evaluation of the

antennas revealed excellent electromagnetic performance, including an average efficiency above 70% and an average gain above 1dBi within the operational frequency band.

Wang et al. developed a wearable microwave breast imaging system with a compact UWB antenna array. The flexible UWB antennas were optimized for size and cost using a thin-film laminate, while a non-stretchable dielectric spacer ensured suitability for wearables [38]. The system consisted of a 3D cylindrical antenna array with 24 antennas, constructed from four 2D circular arrays as illustrated in Figure 5. Operating in the 4.97-11.73 GHz range, the antennas exhibited omnidirectional radiation. Validated with a realistic breast model, the system accurately detected and located 5-mm diameter tumors using the Delay-and-Sum algorithm in Computer simulation technology (CST) simulations.

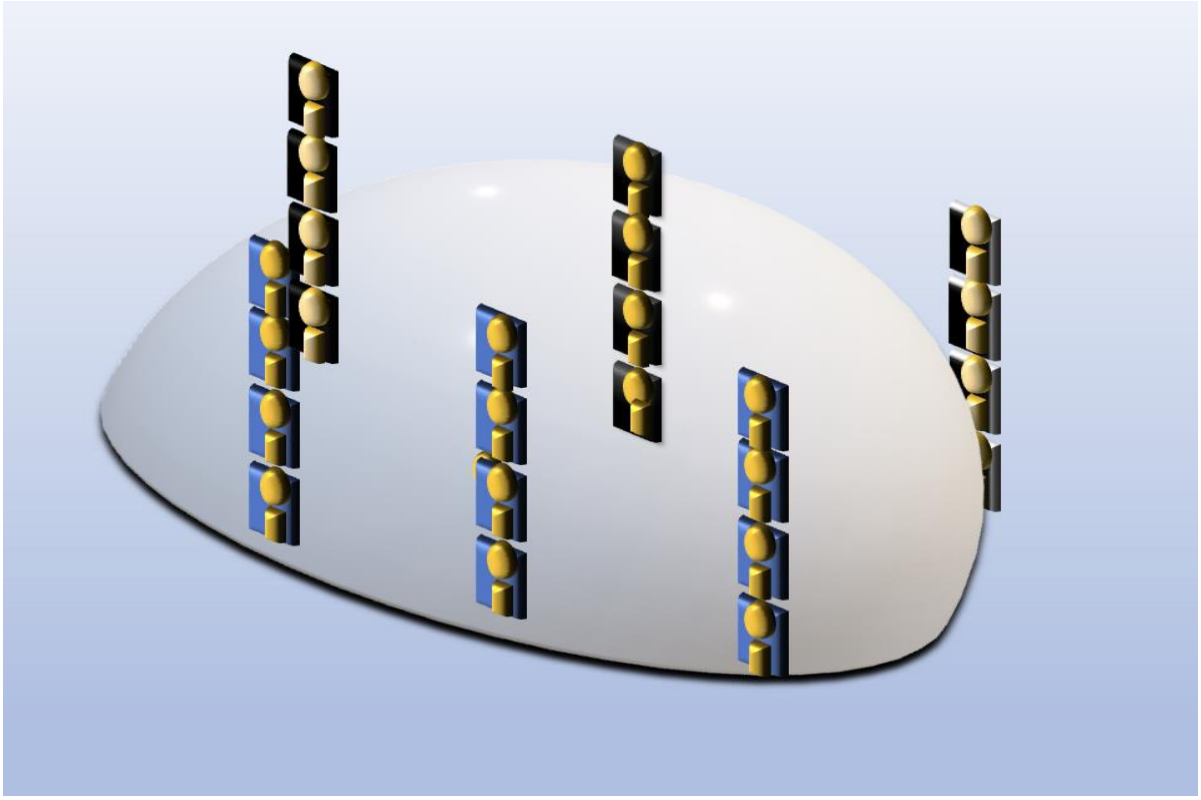

Figure 5. Four-level antenna array mounting on breast model

In a recent study [39], flexible monopole antennas were developed on a cotton substrate for radar-based microwave breast imaging. The antennas exhibited an impedance bandwidth of 2.2-8 GHz and a compact footprint of 50 × 50 mm². Simulations and measurements confirmed their performance near breast models with and without tumors, considering bending capabilities and washing effects. The findings highlight the potential of using fully textile antennas in wearable microwave imaging systems, although their sensitivity to tumors smaller than 5 mm remains a limitation.

Previous studies have demonstrated the suitability of flexible UWB antenna arrays for breast cancer detection, showcasing their potential in improving early detection of small-sized tumors up to 1cm [40]-[43]. Similarly, this master thesis aims to present and evaluate a practical wearable self-monitoring vest equipped with flexible UWB antennas and channel analysis as a proof-of-concept.

2.6 Tissue-Mimicking Phantoms

Tissue-mimicking phantoms play a crucial role in enhancing the accuracy and reliability of Microwave breast imaging systems. The evaluation of these systems' diagnostic capabilities in terms of sensitivity and specificity is vital. However, conducting tests directly on patients without clinical validation is impractical. To address this, layered phantoms that closely resemble the anatomy and electrical properties of human breast tissues are developed. These phantoms accurately simulate different tissue types and their relative electrical properties. It is also important to ensure that these phantoms can be easily reproduced using cost-effective and readily available materials, while prioritizing their safety for use in scientific research [44].

Liquid-based phantoms such as oil dispersions and glycerine are commonly used in existing studies [45]-[46]. However, these materials do not accurately mimic the complexity of real tissues, limiting their suitability for advanced device optimization. To overcome this, numerous research teams worldwide are actively engaged in developing tissue-mimicking materials for breast phantoms. These materials aim to replicate the properties of human breast tissue and can range from simple oil-in-gelatine mixtures to more intricate chemical compositions, including those compatible with 3D printing technology. These improved phantoms will closely resemble actual tissues, enabling better simulations and advancements in device technology [44].

Henin et al. developed an electro-biomechanical breast phantom for testing microwave-mechanical hybrid systems designed for breast imaging [47]. The phantom was fabricated using low-cost materials such as gelatin, water, grape seed oil, propylene glycol, and commercial dishwashing liquid. They created two samples with different oil concentrations, namely 50% and 80%, to achieve varying electrical properties in the artificial tissues. These samples were then subjected to testing using the HP85070 dielectric probe, covering frequencies ranging from 1 to 4 GHz.

Baker et al. developed a heterogeneous breast phantom for testing an UWB Micowave Imaging System (MIS) in early breast cancer detection. They used different materials to represent low- and high-density breast tissues. The low dense phantom consisted of gelatine, grape seed oil, propylene glycol, water, dishwashing liquid, and a cross-linking agent. The highly dense phantom was made from agar powder, vegetable oil, dishwashing liquid, cornflour, and water [48]. The fabricated samples exhibited the required electrical properties, and a hemispherical breast phantom was created for testing the imaging system in the 3 GHz to 11 GHz frequency range.

In [49], the researchers investigated both homogeneous and heterogeneous semi-solid gelatine phantom designs to better understand how breast tissue behaves during microwave imaging. Their study has important implications for improving breast imaging techniques and creating phantoms that closely resemble real breast tissue. However, they encountered inconsistencies in the measured dielectric properties when they varied the oil concentration in the phantoms.

In the study conducted by Islam et al., they developed both homogeneous and heterogeneous breast phantoms to mimic different breast tissue types. The homogeneous phantom was created using a mixture of Sodium chloride, polyethylene powder, agar powder, xanthan gum, sodium dehydroacetate monohydrate, and distilled water. On the other hand, the heterogeneous phantom consisted of distilled water, safflower oil, propylene glycol, 200 bloom calf-skin gelatin, formalin, and a surfactant (xanthan gum). The researchers also employed non-ionic surfactant materials to enhance the durability and preservation of the phantom, ensuring stability of its properties over time [50].

In [51], researchers utilized 3D printing to fabricate solid phantoms in the form of hemispherical shells made of polyurethane rubber combined with graphite and carbon powders. However, the materials used in this study are not commonly found and readily available. The proposed tumor phantom set introduced in the study incorporated various shapes and levels of spiculation, aiming to simulate different degrees of tumor malignancy. It is worth noting that this is the first attempt to incorporate such diverse characteristics into a tumor phantom.

Lazebnik et al. created gelatine-based TM phantoms using a solution of 50% kerosene and 50% safflower oil with a formaldehyde-based emulsion. These phantoms closely mimic the dispersive dielectric properties of various biological tissues across a broad frequency range (500 MHz to 20 GHz) [15]. They enable the formation of heterogeneous and anthropomorphic configurations while maintaining long-term stability in mechanical and electromagnetic properties. Although these materials provide electromagnetic stability over time, their high cost and difficulty in handling pose significant challenges.

Existing solutions for creating breast phantoms have limitations that need to be addressed. The use of toxic ingredients, such as formaldehyde, requires specialized equipment and precautions during handling. Fabrication techniques like 3D printing can be expensive and require advanced equipment [44]. Additionally, the characterization of these phantoms is often limited to specific frequency ranges, which may impact their accuracy. It is important to establish clear guidelines for designing phantoms with desired electromagnetic properties. Overcoming these challenges will contribute to the development of more reliable and improved breast phantoms.

Therefore, this research focuses on the development of heterogeneous breast phantoms using affordable materials and cost-effective production methods. The proposed phantom is designed with multiple layers and a semi-solid structure, incorporating tissue-equivalent materials [52]. These phantoms successfully mimic the electromagnetic behaviour of tissues when exposed to microwaves. To create the desired breast shape, a mold created through 3D printing technology is utilized.

3 PREPARATION OF TISSUE-MIMICKING PHANTOMS

This section provides a comprehensive methodology for preparing tissue phantoms that mimic skin, muscle, fat, tumor, and gland tissues, establishing a solid foundation for subsequent experiments and investigations. Developing a realistic breast tissue-mimicking phantom for mm-wave imaging involves meeting key requirements. It should accurately replicate the dielectric properties of real tissues within the desired frequency range, maintain stable electromagnetic properties over time, and utilize cost-effective and non-toxic materials in production and preservation processes.

The primary objective of this section is to outline a design procedure for creating phantoms capable of accurately mimicking different categories of human breast tissues, encompassing both healthy and cancerous tissues. By achieving this goal, one can effectively simulate and evaluate mm-wave imaging techniques in a controlled and reproducible manner.

3.1 Methodology

The preparation of tissue phantoms encompassed several crucial steps, including ingredient selection, formulation development, fabrication techniques, and stability assessment.

3.1.1 Ingredient Selection

The selection of ingredients was conducted meticulously, considering their ability to effectively mimic the desired properties of the target tissues. This involved the careful selection of gelling agents, solvents, fillers, and additives that closely replicated the dielectric characteristics of the respective human tissues.

3.1.2 Formulation Development

Extensive efforts were made to develop the optimal formulations for the tissue phantoms. Through systematic experimentation, various ratios and concentrations of the selected ingredients were tested to achieve the closest possible resemblance to the dielectric properties of human tissues. This iterative process allowed for the refinement and fine-tuning of the tissue phantom formulations.

3.1.3 Fabrication Techniques

A range of fabrication techniques were employed to ensure the successful creation of tissue phantoms with consistent properties. These techniques involved the careful application of heating, stirring, and molding methods to guarantee the uniform distribution of ingredients within the phantoms. This uniform distribution was crucial for achieving the desired solid-state consistency and stability of the tissue phantoms.

3.1.4 Stability Assessment

To ensure the reliability and reproducibility of the tissue phantoms, comprehensive stability assessments were performed. These assessments involved the rigorous evaluation of the physical and dielectric properties of the phantoms over time. By subjecting the phantoms to

stability tests, their long-term performance and consistency were scrutinized, allowing for the identification of any potential changes or degradation in their properties.

By adhering to this meticulous methodology, tissue phantoms for skin, muscle, fat, tumor, and gland tissues were successfully prepared. The subsequent sections of this thesis will delve into a detailed analysis of the composition, fabrication techniques, and microwave properties of each tissue phantom. This comprehensive exploration will establish a solid groundwork for the utilization of these tissue phantoms in microwave-based studies, facilitating accurate and reliable investigations in various research areas.

3.2 Fat Phantom

This section details the creation of a fat phantom to replicate the microwave properties of fat tissue commonly found in the breast. The objective was to develop an affordable and accessible method for gaining insights into microwave characteristics. This technique has the potential to extend beyond the scope of this study and be applied to other tissues in future microwave research. The detailed description of the fat phantom used in this study was based on the work published in [53], where I contributed as the second author.

3.2.1 Ingredient Selection and Requirements for Fat Phantom

A series of tests were conducted to select suitable ingredients and assess the feasibility of manufacturing the fat phantom. The phantoms needed to fulfill specific requirements, including long-term stability, comparable microwave characteristics to human tissues, and a solid composition for ease of handling during experiments. Through preliminary investigations, it became evident that a fat phantom with lower water content could effectively mimic the electrical properties of fat tissue. However, high concentrations of coconut and sunflower oils proved challenging to homogenize. As a result, a combination of gelatin (as a gelling agent), distilled water, propylene glycol (with low conductivity), dishwashing liquid, and xanthan were selected, with necessary adjustments made to achieve the desired range of conductivities and relative permittivity.

3.2.2 Procedure for Preparation of Fat Phantoms

The following steps were undertaken to prepare the fat phantoms:

1. Distilled water was heated on a hot plate stirrer until reaching approximately 65 °C in a beaker.
2. Gelatin was gently added to the warm water while maintaining a temperature of around 65 °C. The mixture was stirred for approximately 5 minutes.
3. Separately, PG (propylene glycol) was heated to approximately 50 °C.
4. The heated PG was then gradually added to the gelatin-water mixture while continuously stirring until the solution reached 65 °C.
5. Thoroughly combining xanthan with the solution was ensured.
6. Dishwashing liquid was added to the solution and thoroughly mixed as depicted in Figure 6.
7. The solution was poured into an appropriate mold and refrigerated for 24 hours to solidify.
8. Before any measurements were taken, the phantoms were allowed to rest at room temperature for about an hour.

Figure 6. Solution while mixing all the ingredients during the fabrication of phantoms

3.2.3 Composition of Fat Phantoms and Microwave Property Measurements

A comprehensive investigation was conducted to explore the microwave properties of various compositions of gelatin, propylene glycol, xanthan, and dishwashing liquid in the development of fat phantoms. The measurements were carried out using an open-ended coaxial dielectric probe (Dielectric Probe Kit DAK 3.5, SPEAG, Switzerland) connected to a vector network analyzer (VNA) (Keysight Streamline P9375A) [53]. The frequency range of 200 MHz to 8 GHz was swept with 117 points to capture two port scattering parameters.

Prior to the measurements, the calibration process was performed using the standard Open Source Load (OSL) calibration method. This involved three essential measurements: the open measurement, where the probe was held in the ambient air; the short measurement, where the probe was connected to the shorting block; and the load measurement, where the probe was immersed in the calibration liquid "Head" provided by DAK [53]. To ensure the calibration's accuracy, the dielectric properties of the calibration liquid "Head" were compared with the data sheet, serving as a validation step.

After the successful calibration, the measurements were conducted on different trials of the fat phantom (FP) mixture solution at room temperature as shown in Figure 7. Multiple measurements were taken at 2-3 different locations within each sample to obtain a representative average value for the dielectric properties of the fat phantom mixture solution. This approach ensures a reliable and robust assessment of the sample's dielectric properties.

Table 1. Different fat phantom mixture trials and their dielectric properties.

Fat Phantom Trial No.	Concentration of Ingredients					Permittivity/Conductivity		
	Distilled Water	Gelatin	Propylene Glycol	Xanthan	Dishwashing liquid	2.5GHz	6 GHz	8Ghz
FP1	5ml	3g	20ml			10.32/1.3	6.92/1.7	6.19/2.1
FP2	3ml	2g	20ml	1g	0.5ml	9.26/1.12	6.54/1.56	5.88/1.76
FP3	3ml	1.5g	20ml	1g	0.5ml	8.85/1.16	5.98/1.53	5.7/1.87
FP4	2ml	1.5g	20ml	1g	0.5ml	8.56/1.09	6.16/1.50	5.61/1.73
FP5	2ml	1g	20ml	1g	0.5ml	8.15/1.04	5.9/1.40	5.4/1.65
FP6	2ml	0.75g	20ml	2g	0.5ml	7.8/0.9926	5.82/1.28	5.4/1.56
FP7	2ml	0.75g	20ml	1g	0.5ml	7.71/0.98	5.73/1.26	5.29/1.525
FP8	1.5ml	0.75g	20ml	2g	0.5ml	6.84/0.82	5.32/1.05	5/1.284
FP9	1.5ml	0.75g	20ml	1g	0.5ml	7.014/0.85	5.40/1.090	5.06/1.32
FP10	3ml	2g	25ml	1g	0.5ml	7.05/0.85	5.21/1.08	5.01/1.19
FP11	3ml	2g	30ml	1g	0.5ml	7.09/0.85	5.11/1.01	4.95/1.17
FP12	3ml	2g	35ml	1g	0.5ml	7.08/0.85	5.19/1.052	4.93/1.12
FP13	3ml	2g	40ml	1g	0.5ml	6.4/0.75	5.0/0.953	4.76/1.02
FP14	3ml	2g	50ml	1g	0.5ml	6.1/0.73	4.8/0.92	4.5/1.00

The recorded data included the relative permittivity and conductivity of the fat phantom materials at frequencies of 2.5 GHz, 6 GHz, and 8 GHz. The results in Table 1 revealed that increasing the volume percentage of PG led to a decrease in relative permittivity, while reducing the concentration of water resulted in lower conductivity in the aqueous gelatin solution. These findings contribute to a deeper understanding of the microwave behavior of the fat phantom materials and provide valuable insights for their application in breast tissue mimicking.

3.2.4 Results of Various Fat Phantom Trials

The development of various fat-phantom trials was conducted to achieve a mixture solution that closely mimics the properties of real fat tissue. It can be seen from Table 1 that the first trial, FP1, consisted of propylene glycol (20 ml), distilled water (5 ml), and gelatine (3 g). However, Table 1 shows that both the relative permittivity and conductivity values for FP1 were significantly higher than those of real fat tissue, indicating the need for further adjustments.

Subsequent trials, such as FP2, introduced modifications by reducing the amount of water and gelatine while incorporating xanthan and dishwashing liquid. This led to a noticeable decrease in both relative permittivity and conductivity compared to FP1, although they still exceeded the target values for fat tissue emulation. Trials FP3 to FP5 continued to decrease the amount of water and gelatine, resulting in further reductions in relative permittivity and conductivity.

In trials FP6 to FP9, the amount of gelatine was significantly reduced to 0.75 g. However, this reduction did not bring the relative permittivity below 5, and the conductivity remained too high. Insufficient water content made it challenging to dissolve the gelatine completely in these trials.

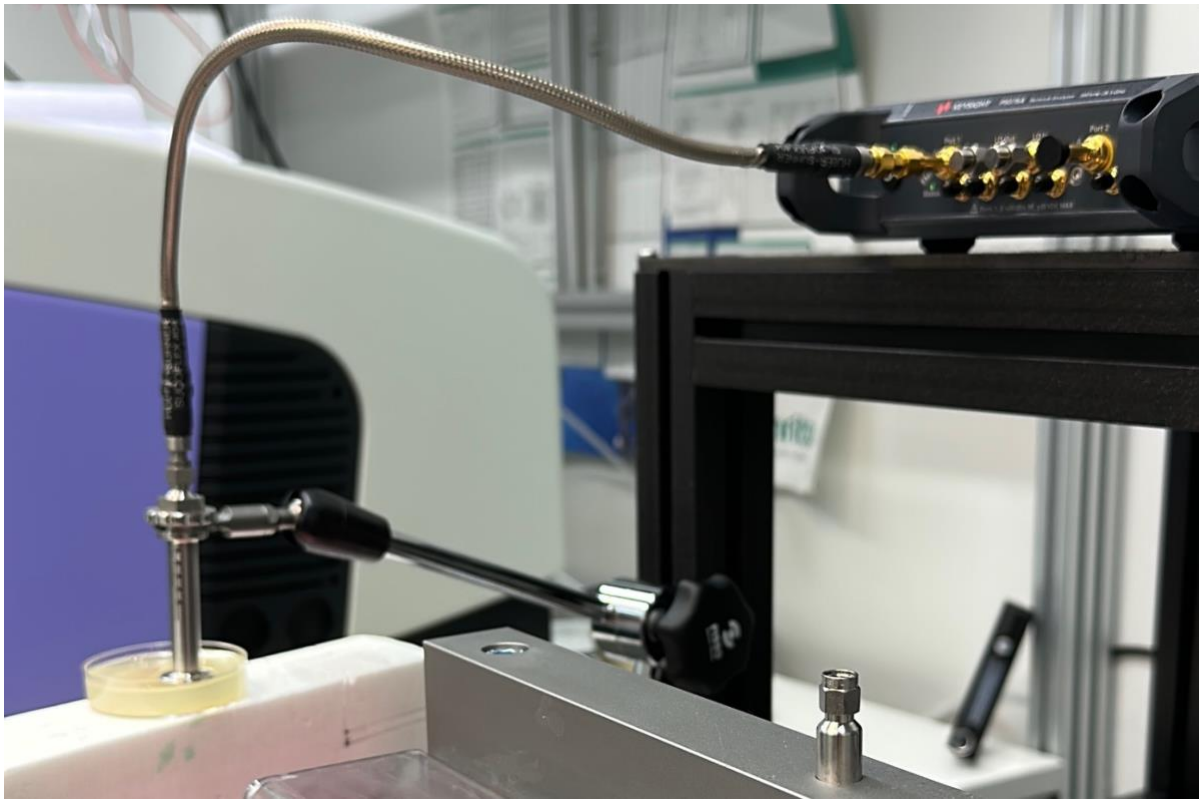

Figure 7. The setup for measuring dielectric properties with VNA and SPEAG's dielectric assessment kit

To evaluate the impact of increasing the amount of propylene glycol, trials FP10 to FP14 were conducted. The addition of propylene glycol necessitated the addition of water, resulting in more moderate decreases in relative permittivity and conductivity values. Notably, FP13 and FP14, which included 40 ml and 50 ml of propylene glycol, respectively, exhibited relative relative permittivity and conductivity values that closely resembled those of real fat tissue. However, FS14 did not fully solidify even after several days, rendering it unsuitable for 3D emulation platforms that require fully solid phantoms.

After conducting several trials, the optimal composition for the fat phantoms was determined to be FP13: 40 ml propylene glycol, 3 ml distilled water, 2 g gelatin, 1 g xanthan, and 0.5 ml dishwashing liquid. This combination exhibited dielectric and mechanical properties that closely resembled those of fat tissue.

3.2.5 Stability Assessment of Fat Phantoms

Gelatin-based phantoms typically have a limited lifespan, especially when no preservatives are used. Even when stored in the refrigerator, mildew can appear within a few weeks. Moreover, as water slowly evaporates from the phantoms over time, the dielectric properties undergo significant changes, and the phantoms gradually dry out.

To assess the stability of the proposed fat phantom over time, the dielectric properties of FP13 were measured at various intervals: 1, 7, 10, 12, and 60 days. The phantom was stored in the refrigerator and measured at room temperature. After 10 and 60 days, the phantom was reheated and resolidified before conducting the measurements.

Table 2 presents the dielectric properties of the phantom at different time points. It can be observed that the dielectric properties only undergo slight changes during the first 16 days. Particularly in the frequency range of 6-8 GHz, the differences in relative permittivity are negligible, with a maximum variation of 0.2. The variation in conductivity is 0.1 S/m. At lower frequency ranges, the difference in relative permittivity is 0.5, and the conductivity difference is 0.45.

During the initial 10 days, there is a slight decrease in relative permittivity. Reheating the phantom slightly alters its dielectric properties, resulting in a rise of 0.4 units in relative permittivity at the lower frequency range and a rise of 0.1 units at the higher frequency range. The differences in conductivity values remain consistent at 0.1 S/m across the entire frequency range.

Table 2. Dielectric properties for fat phantom after 1,7,10, 12 and 60 days after preparation.

Time-dependent measurements	**Permittivity /Conductivity**					
	Sample1			**Sample 2**		
	2.5GHz	**6 GHz**	**8Ghz**	**2.5GHz**	**6 GHz**	**8Ghz**
on the following day	7.3/0.99	5.23/1.232	5.0/1.317	7.3/0.925	5.4/1.18	5.168/1.26
After 7 days	7.06/0.89	5.26/1.135	4.91/1.203	6.3/0.77	4.803/1.05	4.51/1.13
After 10 days	6.62/0.84	5.07/0.964	4.89/1.108	7.55/0.98	5.44/1.21	5.14/1.34
After melting at 60°C and forming back again at day 12	6.78/1.176	5.17/1.123	5.09/1.08	7.6/0.98	5.49/1.19	5.22/1.32
After 60 days melting at 60°C and forming back again	6.6/0.8252	5.04/1.09	4.764/1.1	7.09/0.93	5.28/1.16	4.92/1.26

After 60 days, the dielectric properties of the phantoms exhibit more significant changes. The relative permittivity increases by 0.5-1 units, and the conductivity decreases by 0.1-0.45 S/m. These observations indicate that over an extended period, the dielectric properties of the phantoms are notably affected.

Overall, the stability analysis reveals that the proposed fat phantom experiences only minimal changes in dielectric properties within the first 10 days. However, after a prolonged period of 60 days, more substantial variations in relative permittivity and conductivity are observed. However, further research is recommended to increase the concentration of propylene glycol for better replication of the microwave characteristics of fat tissue in the breast.

3.2.6 Summary of Material Preparation and Measurements for Fat Phantoms

In summary, this section introduced a robust and innovative fat tissue phantom suitable for lower microwave frequency ranges. By utilizing pure propylene glycol as the primary ingredient, the phantom demonstrated dielectric properties that closely resembled those of actual fat tissue. The development process involved meticulous adjustments of ingredients, considering the challenges posed by jellying agents and the necessity of achieving a fully solid solution after polymerization, while maintaining the desired dielectric properties.

Extensive evaluations and comparisons were conducted to validate the effectiveness of the proposed solid phantom. The results revealed excellent agreement between the phantom and real fat tissue, particularly within the frequency range of 6 GHz to 10 GHz, where the differences were negligible. The most significant deviations were observed at 2.5 GHz. Even at lower ultrawide band frequencies (below 5 GHz), the disparities in relative permittivity and conductivity were relatively small, ranging from 0.4 to 0.8 and 0.1 to 0.2, respectively.

By addressing the complexities of mixing jellying agents with propylene glycol and achieving a solid fat tissue phantom with accurate dielectric properties, this research offers a valuable tool for microwave-based investigations and applications in the field of medical diagnostics. The close resemblance of the phantom to real fat tissue enables improved evaluation and validation of microwave imaging techniques for detecting and diagnosing fat-related abnormalities and diseases.

The developed fat tissue phantom contributes to the advancement of medical imaging technologies, providing researchers and practitioners with a reliable and versatile tool for testing and refining microwave-based methodologies. It opens up new avenues for enhancing the accuracy and reliability of fat tissue imaging, ultimately leading to improved diagnostic capabilities and better patient outcomes.

3.3 Skin and Tumor Phantoms

The objective of this study was to develop skin and tumor phantoms that accurately mimic the electromagnetic properties of human skin and tumor tissues. Through careful formulation and evaluation, reliable models were successfully created for investigating microwave behaviors in skin and tumor studies.

3.3.1 Skin and Tumor Phantom Preparation

The skin and tumor phantom materials were prepared using a similar procedure as the fat phantom. The reagents, including distilled water, gelatin, sunflower oil, and dishwashing liquid, were measured accurately using high-precision scales.

For the gelatin-based phantoms, deionized water was gradually heated to approximately 65°C while stirring the mixture on a magnetic hot-plate stirrer. The gelatin was added and stirred until completely dissolved. Following this, dishwashing liquid and sunflower oil were introduced to the water-gelatin solution, resulting in a clear emulsion that appeared homogeneous, dense, and pale in color. The stirring process was continued for approximately five minutes to ensure proper mixing.

Once the mixture reached a temperature of about 50°C, it was removed from the hot plate while maintaining continuous stirring. The solution was then carefully poured into molds and allowed to polymerize. The molds with the solution were refrigerated for 3.5 hours to facilitate solidification.

Before conducting any measurements, the phantoms were allowed to rest at room temperature for approximately one hour to stabilize. This resting period ensured that the phantoms were in a consistent state for subsequent evaluations and analyses.

3.3.2 Measurement Analysis and Summary for Skin and Tumor Phantoms

The skin and tumor phantoms were successfully prepared using the aforementioned procedure. Through a series of trials and adjustments in ingredient concentrations, optimal compositions were identified for both skin and tumor phantoms as shown in Table 3 and Table 4.

Several trials were conducted to create tumor phantoms that closely imitate real tumor tissue. The initial trial, TS1, consisted of distilled water, gelatine, sunflower oil, and dishwashing liquid . However, the relative permittivity values for TS1 were significantly lower than those of real tumor tissue, indicating the need for further adjustments. Additionally, the mixture had an excessively oily and liquid consistency, failing to solidify properly.

Table 3. Different Tumor and skin phantom mixture trials with their recipes

Phantom Type	**Sample Trial**	**Concentration of ingredients**			
		Water (ml)	**Gelatin (g)**	**Oil (ml)**	**Dishwasher (ml)**
Tumor	TS1	22	1.7	4.25	0.95
	TS2	8	1.7	4.25	0.95
	TS3	12.3	1.63	1.1	0.9
	TS4	14.3	1.63	1.1	0.9
	TS5	16.3	1.63	1.1	0.9
	TS6	18.3	1.63	1.1	0.9
	TS7	20.3	1.63	1.1	0.9
	TS8	22.3	1.63	1.1	0.9
Skin	SS1	6	3.01	1.68	0.83
	SS2	8	3.01	1.68	0.83
	SS3	10	3.01	1.68	0.83

Subsequent trials, like TS2, attempted to address the issue by reducing the water content to promote solidification. However, the mixture remained excessively oily. Although TS2 showed a decrease in relative permittivity compared to TS1, it didn't resolve the consistency problem.

To improve the mixture, trials TS3 to TS8 were conducted. These trials involved reducing the amount of oil and slightly decreasing the gelatine while increasing the water content in each trial. These adjustments led to a progressive increase in relative permittivity values. Notably, TS7, which contained 20.3 ml of distilled water, exhibited relative permittivity and conductivity values that closely resembled those of real tumor tissue. Moreover, TS7 successfully achieved the desired solid consistency.

Based on the findings from the tumor-phantom trials, the optimal composition was determined to be 20.3 ml of distilled water, 1.63 g of gelatine, 1.1 ml of sunflower oil, and 0.9 ml of dishwashing liquid. This specific combination closely replicated the dielectric and mechanical properties of actual tumor tissue.

Similarly, for the skin phantoms various trials were conducted as seen from Table 3, and the optimal composition was found to be 10 ml distilled water, 3.01 g gelatin, 1.68 ml sunflower

oil, and 0.83 ml dishwashing liquid. The prepared skin and tumor phantoms were measured at different time intervals at 2.5G Hz and 6 GHz, and it was observed that they remained stable and reliable for a duration of up to one week as depicted in Table 4. This durability allows for extended experimentation and analysis without significant changes in their dielectric properties.

In conclusion, the developed skin and tumor phantoms provide valuable tools for investigating microwave characteristics in skin and tumor tissues. Their composition closely mimics the properties of their respective tissues, enabling accurate and controlled experiments. These phantoms offer promising opportunities for further research in the field of microwave applications and hold potential for advancing our understanding of various biomedical phenomena.

Table 4. Different Tumor and skin phantom mixture trials and their dielectric properties after 5 hours, 24 hours, 1 week and 10 days

Phantom Type	**Sample Trial**	**Permitivitty/Conductivity**							
		After 5 hours		**After 24 hours**		**After 1 Week**		**After 10 days**	
		2.5 GHz	**6 GHz**	**2.5 GHz**	**6 GHz**	**2.5 GHz**	**6 GHz**	**2.5 GHz**	**6 GHz**
Tumor	TS1	43.2/1.38	38.6/4.97	41.06/1.08	36.61/4.26	40.8/1.36	36.96/4.99	38.06/1.56	33.3/4.32
	TS2	28.4/2.87	24.6/3.16	28.7/2.81	24.6/3.63	29.3/2.145	24.31/3.62	25.3/1.98	20.6/3.13
	TS3	31.7/1.23	29.2/3.9	31.2/1.12	29.7/4.11	30.9/1.3	28.2/4.16	21.2/1.31	18.5/4.8
	TS4	38.7/1.03	35.12/4.23	38.92/1.04	34.27/4.09	38.7/1.122	33.21/4.03	37.92/1.02	26.25/3.98
	TS5	42.27/1.24	37.51/4.52	43.12/1.32	39.21/5.0	42.27/1.43	38.13/5.1	39.18/1.13	31.42/4.82
	TS6	49/1.45	45.2/5.53	50.9/1.46	45.27/5.6	50.34/1.54	43.52/5.34	40.4/1.32	39.7/4.99
	TS7	62.8/1.68	59.0/6.32	62.9/1.69	57.2/6.52	61.01/1.48	56.47/6.13	57.3/1.21	48.6/5.82
	TS8	70.5/1.75	67.3/6.84	69.0/1.75	63.1/7.16	69.51/1.48	61.26/6.951	61.1/1.83	56.4/6.27
Skin	SS1	30.07/0.93	26.37/3.2	35.07/0.08	27.14/2.15	29.86/1.655	25.12/3.478	20.26/0.54	17.25/2.12
	SS2	35.1/1.34	31.7/3.36	38.9/1.07	32.8/3.12	41.39/1.72	31.96/5.38	23.5/1.82	18.7/2.28
	SS3	40.3/1.48	36.9/4.78	38.2/1.96	34.1/3.76	41.22/1.54	34.11/5.51	30.1/0.93	26.37/3.2

3.4 Glandular Phantom Preparation and Longevity

The glandular phantom, an essential component in simulating glandular tissue for research purposes, was prepared using a controlled procedure. Deionized water was heated to 65°C on a magnetic hot-plate stirrer. Gradually, gelatin was added and stirred continuously until fully

dissolved, resulting in a clear solution. Sugar was then added to the mixture, which was continually stirred. The heat was turned off, and the temperature was allowed to cool to approximately 50°C while maintaining constant stirring. The mixture was then poured into a mold for polymerization. Afterward, the phantoms were refrigerated for 3.5 hours and allowed to rest at room temperature for one hour before use.

Table 5. Glandular phantom recipe and its dielectric properties after 5 hours, 24 hours, 1 week and 10 days.

Concentration of ingredients			**Permitivitty/Conductivity**											
Water (ml)	**Gelatin (g)**	**Sugar (g)**	**After 5 hours**			**After 24 hours**			**After 1 Week**			**After 10 days**		
			2.5 GHz	**6 GHz**	**8GHz**	**2.5 GHz**	**6 GHz**	**8GHz**	**2.5 GHz**	**6 GHz**	**8GHz**	**2.5 GHz**	**6 GHz**	**8GHz**
252	50.5	5.25	62.03/2.03	50.95/8.23	44.75/12.8	61.82/2.15	50.78/8.03	45.39/11.58	62.45/2.15	51.44/8.36	48.11/12.25	57.1/2.02	50.7/8.34	44.99/12.96

To assess the longevity of the glandular phantoms, their stability was monitored over time. The results revealed that these phantoms maintain their properties for up to 10 days as depicted in Table 5, demonstrating their durability and suitability for extended research studies. This prolonged duration ensures consistent and reliable simulations of glandular tissue, providing researchers with ample time to conduct multiple experiments without compromising the integrity of the phantoms.

In conclusion, the carefully prepared glandular phantoms offer a robust and realistic solution for simulating glandular tissue. With their extended longevity and stable properties, these phantoms serve as invaluable tools for various research investigations, enabling accurate and consistent outcomes in the study of glandular tissue.

3.5 Muscle Phantom Preparation and Longevity

The fabrication process for the muscle phantom involved the creation of a saline solution using NaCl in distilled water, which was heated to approximately 65°C on a magnetic hot plate stirrer. Gelatin was gradually added to the heated solution while stirring continuously, ensuring complete dissolution and clarity of the mixture. To enhance the homogeneity of the phantom, dishwashing liquid and sunflower oil were introduced to the saline-gelatin solution once it became clear. After stirring for approximately 5 minutes, the heat was turned off, and the mixture was poured into a mold and refrigerated for about 3 hours until it solidified.

The resulting muscle phantom closely emulates the electrical properties and composition of muscle tissue, making it a valuable tool for research and experimentation. It provides a realistic model for studying the behavior of muscle tissue under various conditions and can be utilized in the development and testing of medical devices and imaging techniques.

Table 6. Muscle phantom recipe and its dielectric properties after 5 hours, 24 hours, 1 week and 10 days.

Concentration of ingredients					**Permitivitty/Conductivity**											
Water (ml)	**Gelatin (g)**	**Oil (ml)**	**NaCl (ml)**	**Dish washer (ml)**	**After 5 hours**			**After 24 hours**			**After 1 Week**			**After 10 days**		
					2.5 GHz	**6 GHz**	**8 GHz**	**2.5 GHz**	**6 GHz**	**8 GHz**	**2.5 GHz**	**6 GHz**	**8 GHz**	**2.5 GHz**	**6 GHz**	**8 GHz**
200	60.2	33.6	166.6	16.6	54.98/1.75	48.9/5.63	45.7/8.2	55.1/1.8	48.59/5.399	45.34/8.6	54.79/1.91	47.99/5.12	45.1/8.59	51.84/3.67	45.1/7.63	43.3/10.2

It is important to note that the stability and longevity of the muscle phantom are crucial considerations. Based on evaluations, it has been determined from Table 6, that the muscle phantom remains suitable for use for a duration of approximately 7 days. This time frame ensures that the phantom maintains its desired characteristics and can reliably simulate muscle tissue throughout experimental procedures.

To preserve the stability of the muscle phantom, appropriate storage conditions, such as refrigeration, should be maintained. Regular assessments and measurements should be conducted to monitor any potential alterations in the phantom's properties over time.

By following the outlined fabrication process and taking into account the stability of the muscle phantom, researchers can confidently utilize this phantom to investigate and gain insights into the behavior and characteristics of muscle tissue in their research endeavors.

4 FINAL BREAST PHANTOM FOR VEST EVALUATION

The final heterogeneous breast phantom assembly for vest measurement consisted of four molds, representing different breast classes: two small molds (diameter d=14cm) and two large molds (diameter d=18cm). Each breast phantom was composed of an outer and inner mold. The outer molds were designed to resemble a prone human breast and were used to create the desired breast shape.

The experimental procedure involved two breast density types: Class IV, which represented very dense breasts challenging for tumor detection with mammography, and Class II, which represented less dense breasts with scattered fibro glandular tissue.

4.1 Class IV (Dense) Breast Phantom

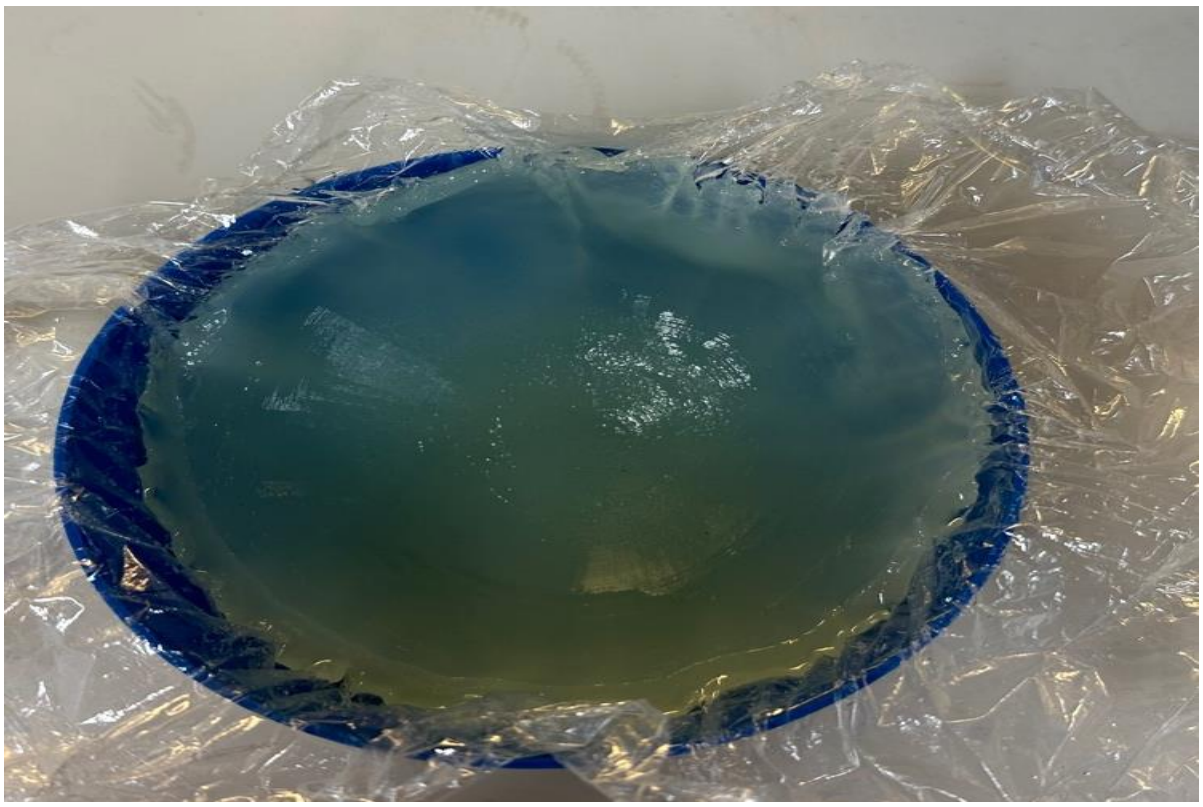

Figure 8. 0.5 cm thick fat layer for Class IV phantom with 14 cm outer mold

To fabricate Class IV phantoms (dense), a specific procedure was followed. An inner mold with a diameter of 13cm was inserted into two different outer molds with diameters of 14cm and 18cm. The outer molds were then filled with a liquid fat material, which solidified into a dome shape as it cooled down as shown in Figure 8. After allowing the fat material to solidify properly by refrigerating it for 24 hours, the inner container was carefully removed.

Next, to create reference glandular tissue, a glandular liquid was poured into the inner mold as depicted in Figure 9. Tumors as shown in Figure 10, measuring 1cm and 2cm were partially inserted into the glandular liquid.The entire assembly was refrigerated for an additional 2 hours. During this time, the glandular liquid and tumors underwent further solidification and integration.

After the additional refrigeration period, more glandular liquid was poured on top of the tumors. The assembly was refrigerated for another 2 hours, allowing the additional glandular liquid to solidify. The resulting solidified glandular phantom with the embedded tumors was then positioned at the center of the previously prepared fat phantom, as depicted in Figure 11 and Figure 12.

This fabrication process ensures the creation of Class IV phantoms with dense breast tissue characteristics. The use of different-sized molds, the solidification of fat and glandular materials through refrigeration, and the precise placement of tumors within the glandular phantom contribute to the realistic representation of dense breast tissue in the resulting phantom structure.

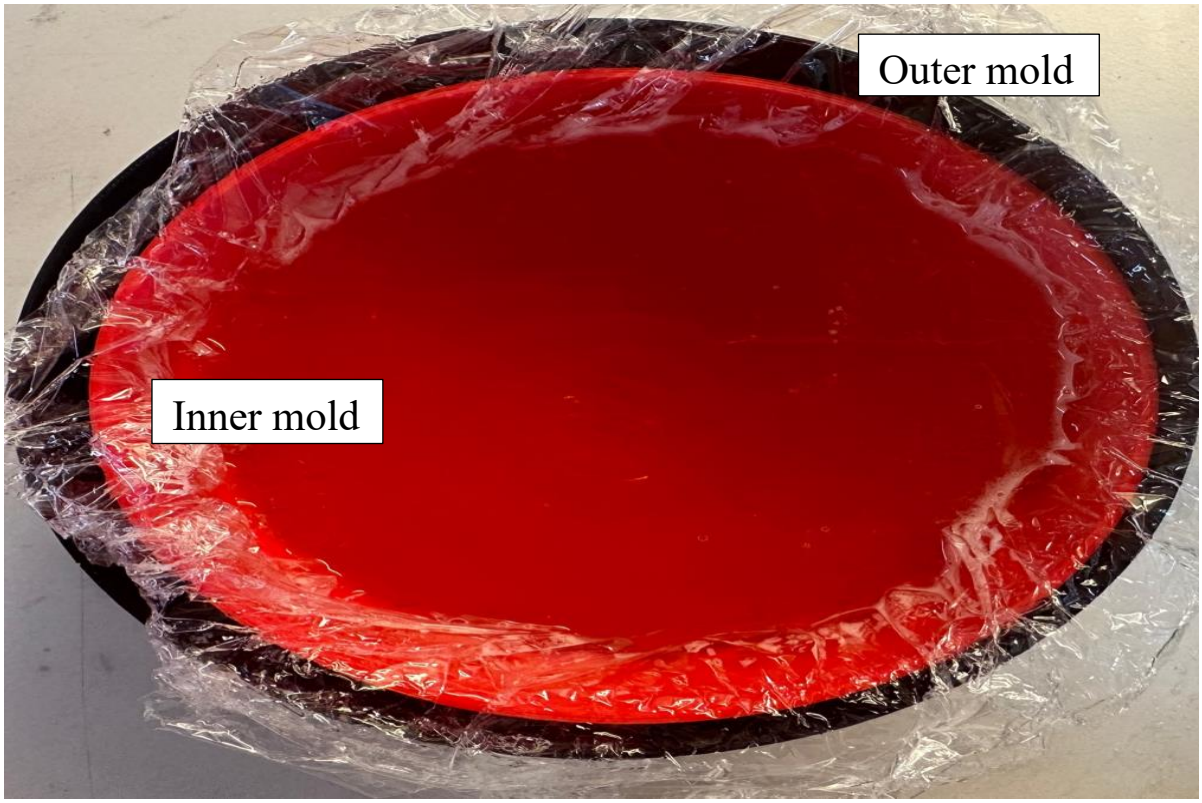

Figure 9. Glandular mixture poured in inner mold for Class IV phantom

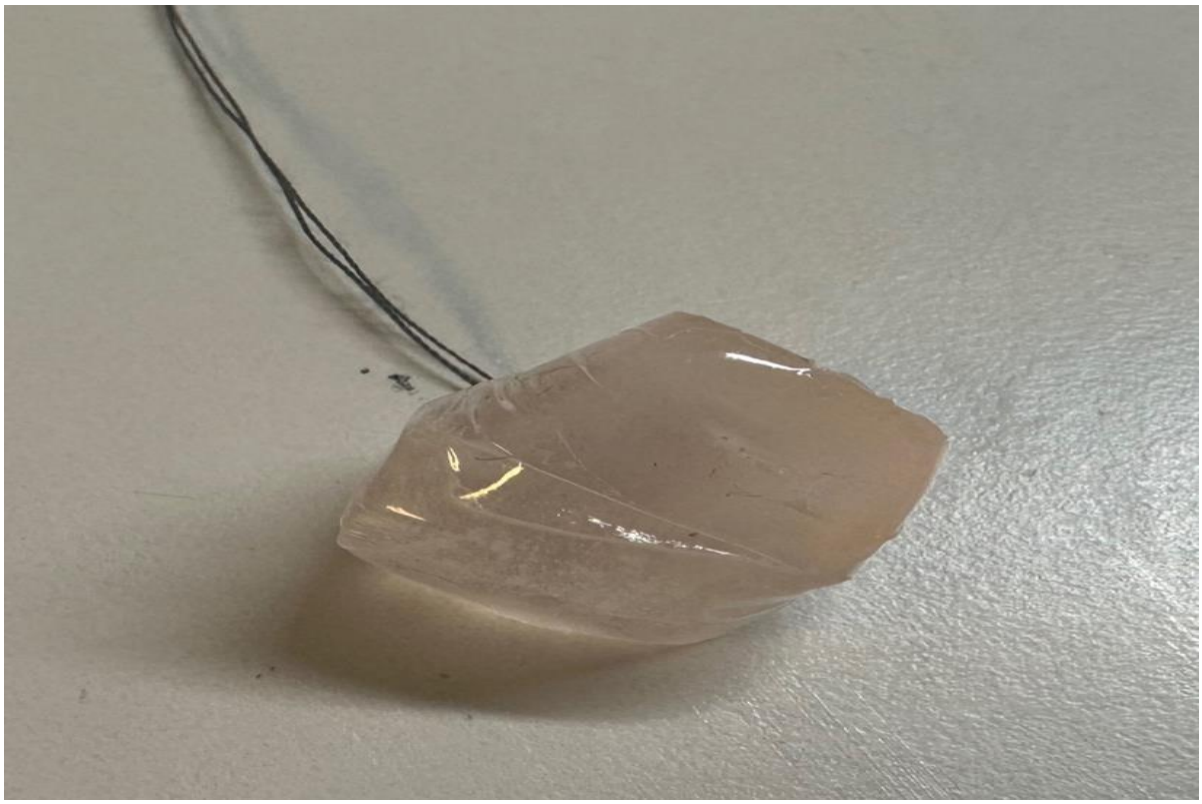

Figure 10. 1 cm Tumor wrapped in a plastic

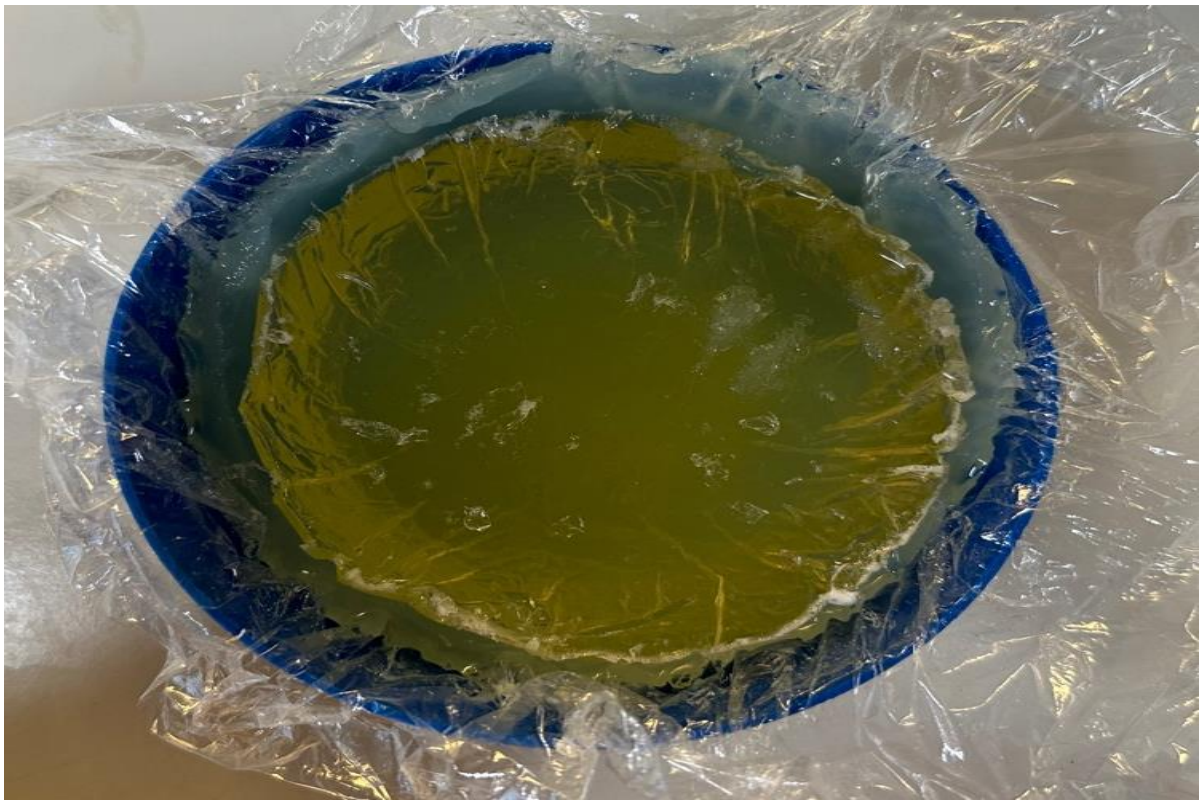

Figure 11. Fabricating Class IV breast phantom in 14 cm outer mould: Dense glandular phantom with 0.5cm thick fat layer

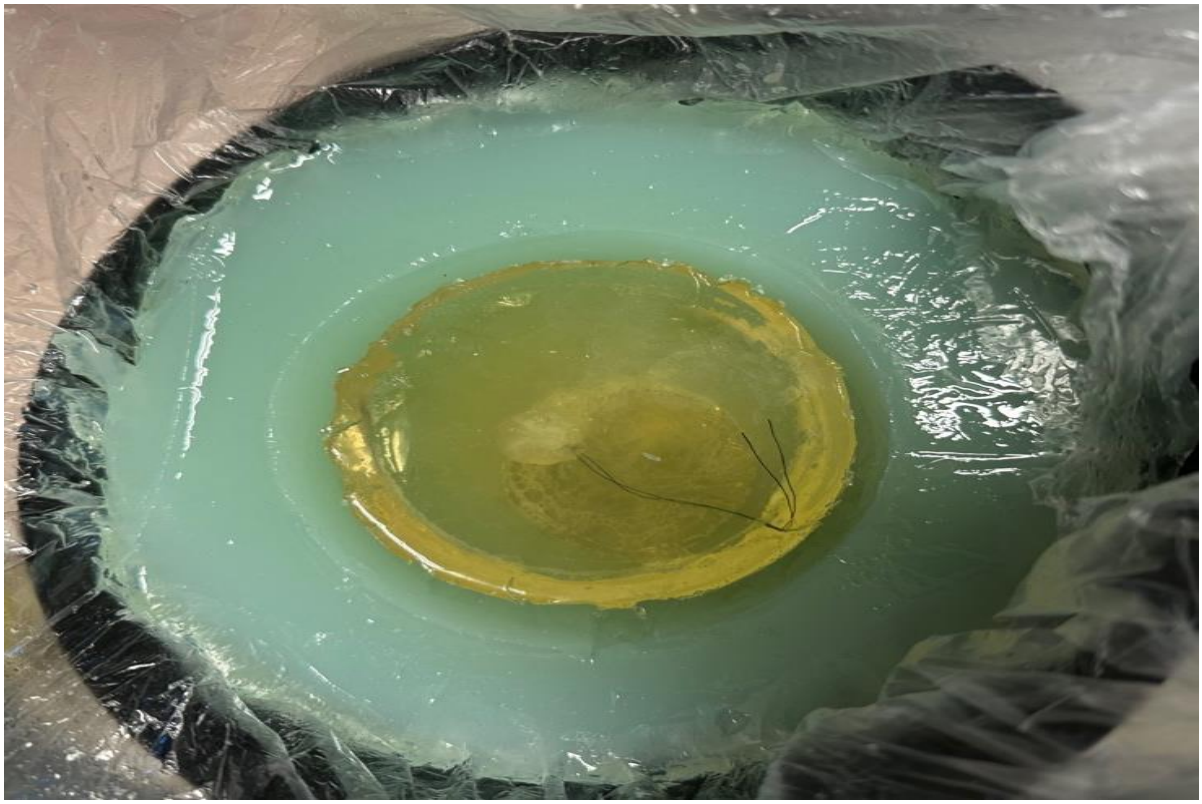

Figure 12. Fabricating Class IV breast phantom in 18 cm outer mould: Dense glandular phantom with 2 cm thick fat layer

4.2 Class II (Less Dense) Breast Phantom

To create Class II phantoms (less dense), the fabrication process involves the following steps. As shown in Figure 14, the outer molds are filled with a liquid fat material, which is then left to solidify over a period of 24 hours. This solidification process ensures that the fat phantom attains the desired shape and consistency.

Next, three cylindrical glandular molds, each measuring 3 x 2 cm and wrapped in thin plastic as shown in Figure 13, are inserted into the solidified fat phantom, as shown in Figure 14. These glandular molds mimic the characteristics of less dense breast tissue.

During measurements, one of the reference glandular molds is replaced with a tumor mold. In one scenario, a tumor mold measuring 1 cm in diameter is inserted into the glandular phantom, while in another scenario, a larger tumor mold measuring 2 cm in diameter is used. This replacement allows for the evaluation and comparison of different tumor sizes within the less dense breast tissue phantom.

By employing this fabrication process, Class II phantoms with less dense breast tissue characteristics can be accurately simulated. The use of fat liquid for the outer molds, the insertion of glandular molds, and the inclusion of tumor molds enable researchers to study and analyze various scenarios relevant to less dense breast tissue imaging and detection.

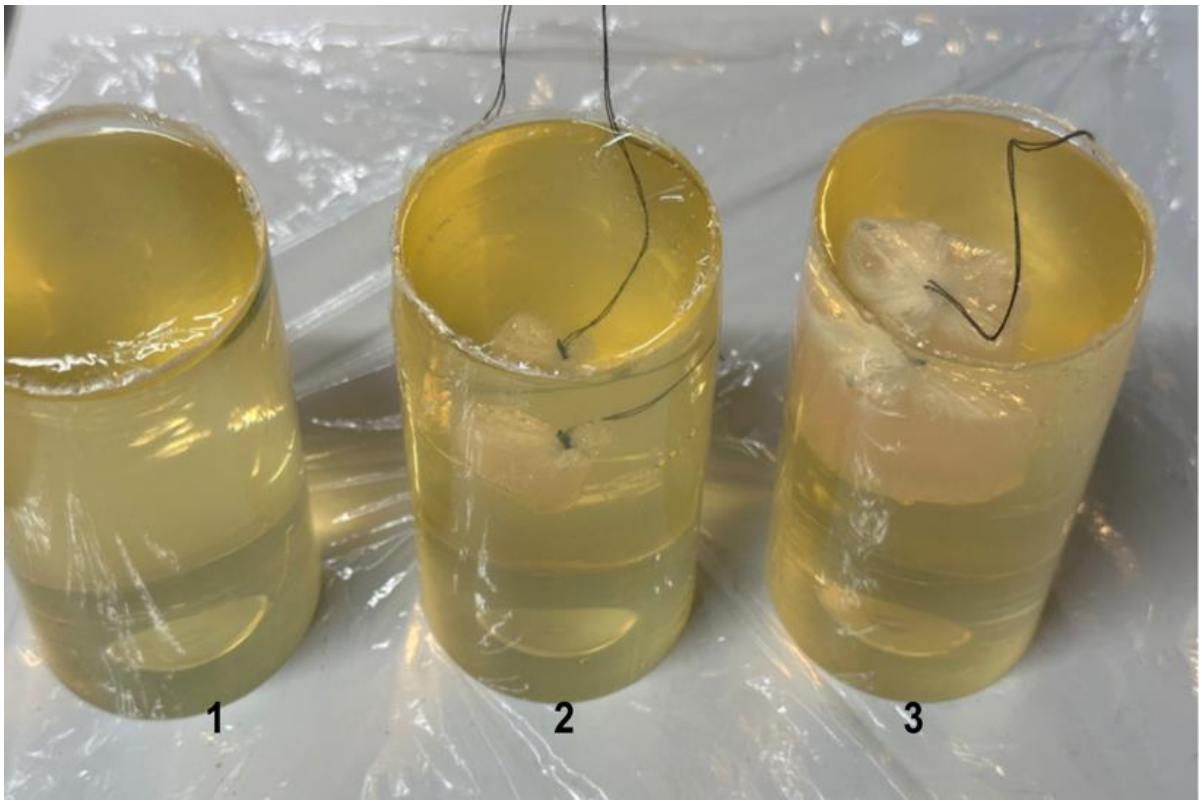

Figure 13. Three cylindrical-shaped glandular phantoms: (1) reference, (2) with 1 cm tumor, and (3) with a 2 cm tumor

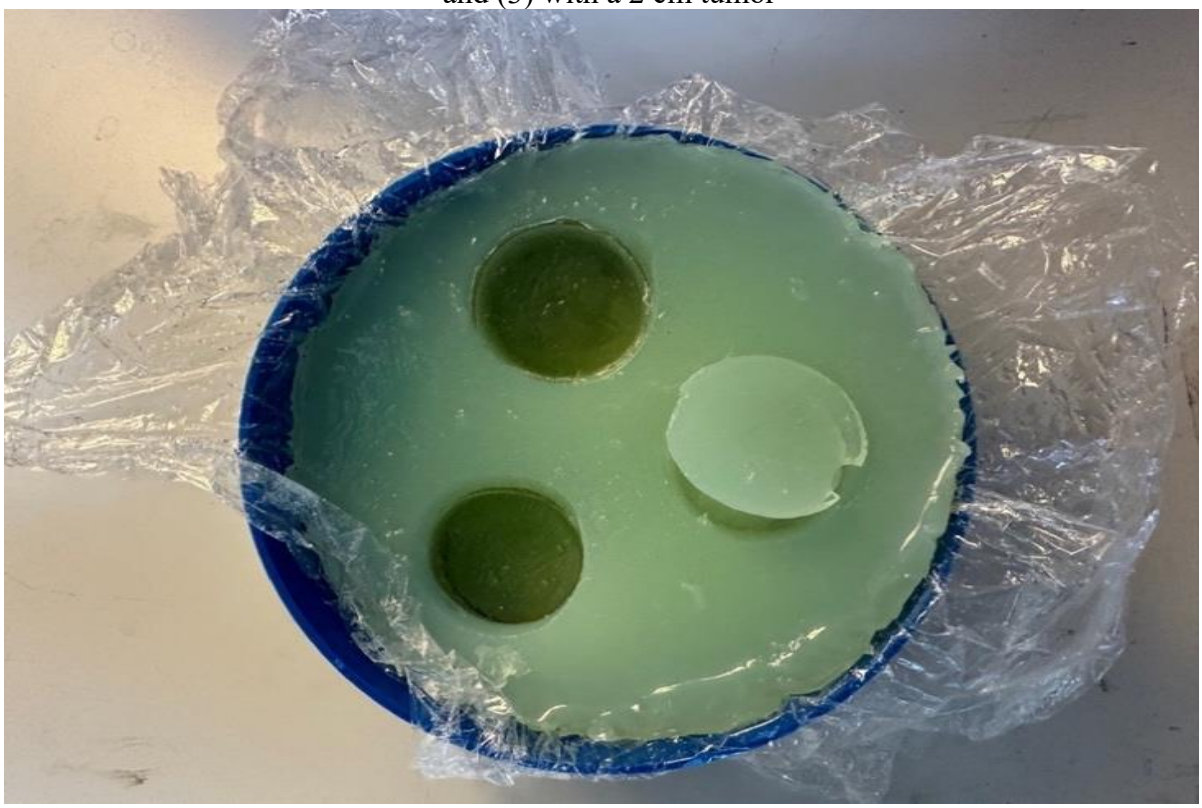

Figure 14. Fabricating Class II Breast phantom, 3 the glandular phantoms inserted into the fat phantom.

4.3 Final Breast Phantom Assembly

To achieve a comprehensive breast phantom assembly, two additional layers were incorporated. Firstly, a 0.6 mm thick skin layer was carefully placed on the outer surface of the fat layer. This layer simulated the texture and appearance of the skin, enhancing the realism of the phantom. Secondly, a 1.5 mm thick muscle layer was positioned at the base of the fat layer, replicating the underlying muscle tissue commonly found in a natural breast structure.

By incorporating these layers, the breast phantom assembly accurately mimicked the composition and structure of a real breast. This realistic representation was essential for conducting precise measurements and evaluating the performance of a specialized vest designed for tumor detection across varying breast densities. The complete setup, which included the vest and phantoms positioned on a mannequin torso, is illustrated in Figure 15.

The heterogeneous breast phantom assembly provided a valuable tool for assessing the effectiveness of the vest under different breast conditions. It facilitated accurate measurements and evaluation of the vest's performance in detecting tumors within breast tissues of varying densities. This assembly played a significant role in advancing breast imaging research and development, contributing to the refinement of tumor detection techniques and the improvement of breast health outcomes.

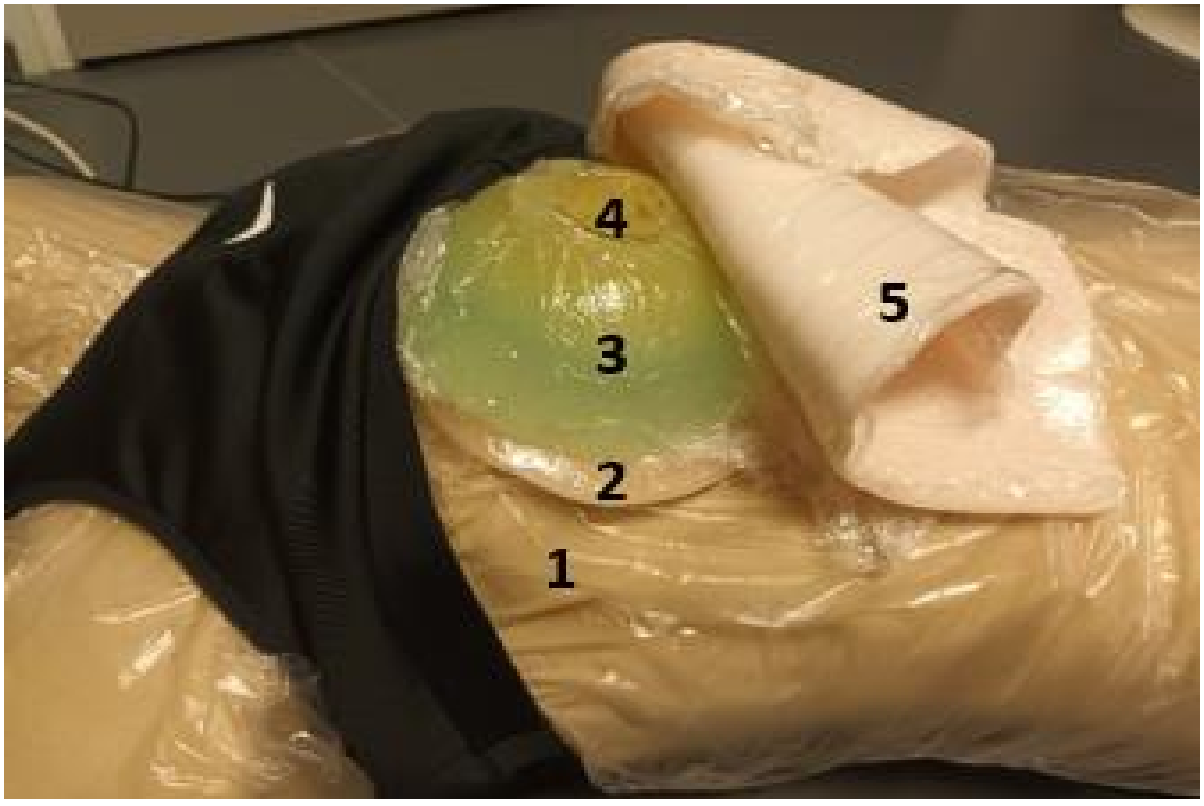

Figure 15. The measurement setup with phantoms set on the mannequin torso (1), above which the muscle layer is first assembled (2), fat phantom (3), glandular tissue phantom(4) skin phantom(5)

5 MONITORING VEST

5.1 Antennas

The tumor detection vest incorporates three different antennas: Antenna1, Antenna2, and Antenna3.

5.1.1 UWB Monopole Antenna with Flexible Laminate Substrate

Antenna1 is a UWB monopole antenna with a flexible laminate substrate, initially designed for in-body sensing in the 2-10 GHz frequency range [54]. It has dimensions of 2cm x 3cm and provides wideband coverage for tumor detection as shown in Figure 16.

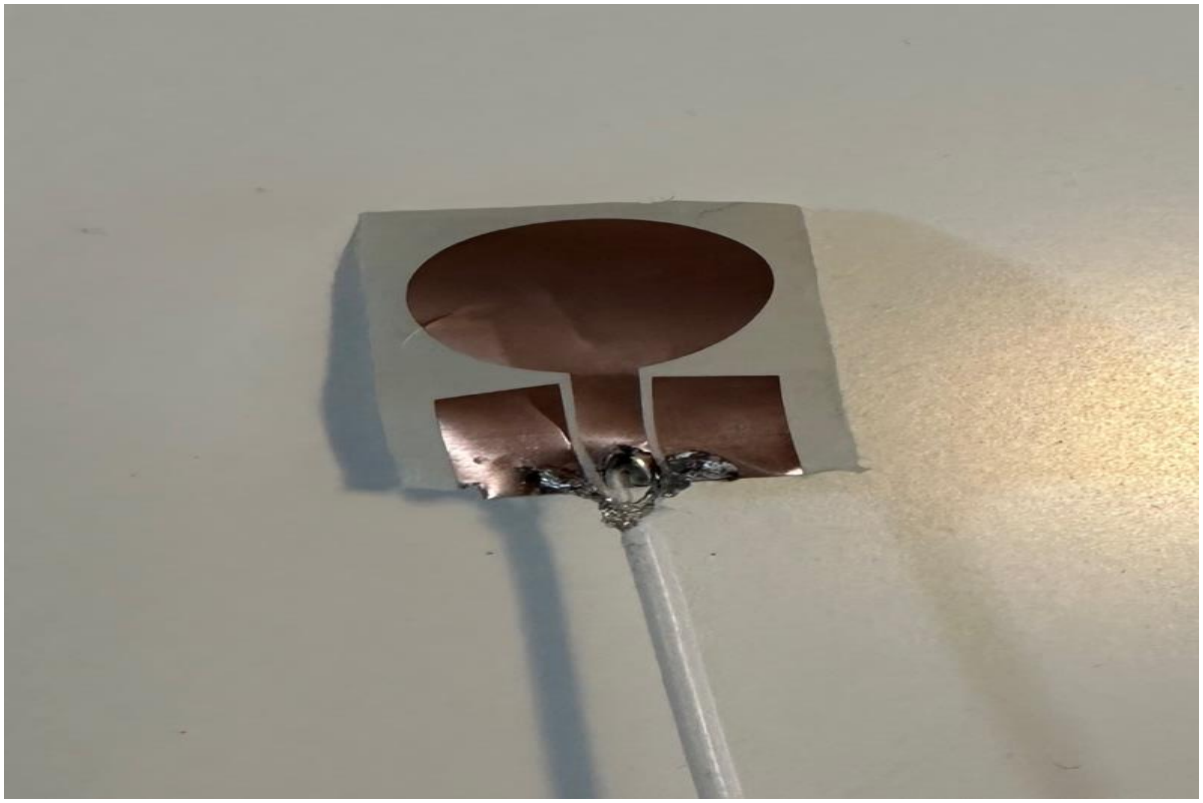

Figure 16. UWB monopole antenna with flexible laminate substrate (Antenna 1)

5.1.2 UWB Monopole Antenna with Conductive Textile Substrate

Antenna2 is a textile-based version of Antenna1 as depicted in Figure 17. It is fabricated using assisted laser etching techniques to define the antenna pattern on a separate textile substrate as shown in Figure 18.

The LPKF ProtoLaser U3 machine is employed to perform the precise etching process, ensuring accurate pattern creation on the textile material. This enables seamless integration of the antenna into wearable electronics and smart textiles. Antenna2 shares the same design and characteristics as Antenna1, ensuring consistent performance while allowing for integration into the vest.

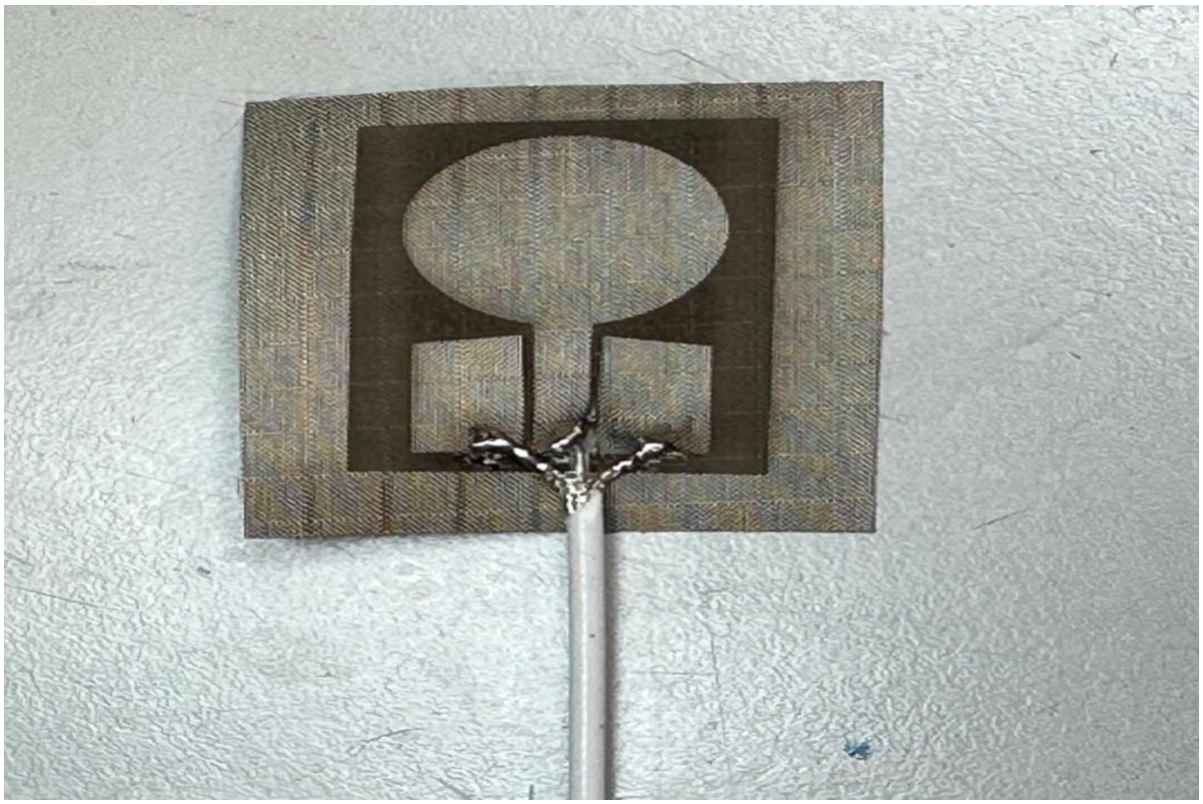

Figure 17. UWB monopole antenna with conductive textile (Antenna 2)

5.1.3 UWB Monopole 2 (Larger) Antenna with Kapton Polyamide Substrate

Antenna3 in Figure 19, on the other hand, features a Kapton-based substrate and has slightly larger dimensions than Antenna1 and Antenna2. With dimensions of 4cm x 4cm, Antenna3 incorporates a larger radiator to improve radiation characteristics towards the body.

The Antenna3 fabrication process begins with the selection of a 50-um flexible Kapton polyamide substrate, known for its thermal stability and electrical insulation properties, making it suitable for antenna applications. The first step in the process involves screen printing a square pattern onto the Kapton material using an EKRA screen printing machine.

Screen printing is a widely used technique that involves pressing ink through a fine mesh screen onto the material, transferring the desired pattern onto the substrate [56]. In this case, a specially designed screen with an open area corresponding to the square pattern is used. The ink used is DuPont 5964H silver ink, which offers good conductivity for the antenna.

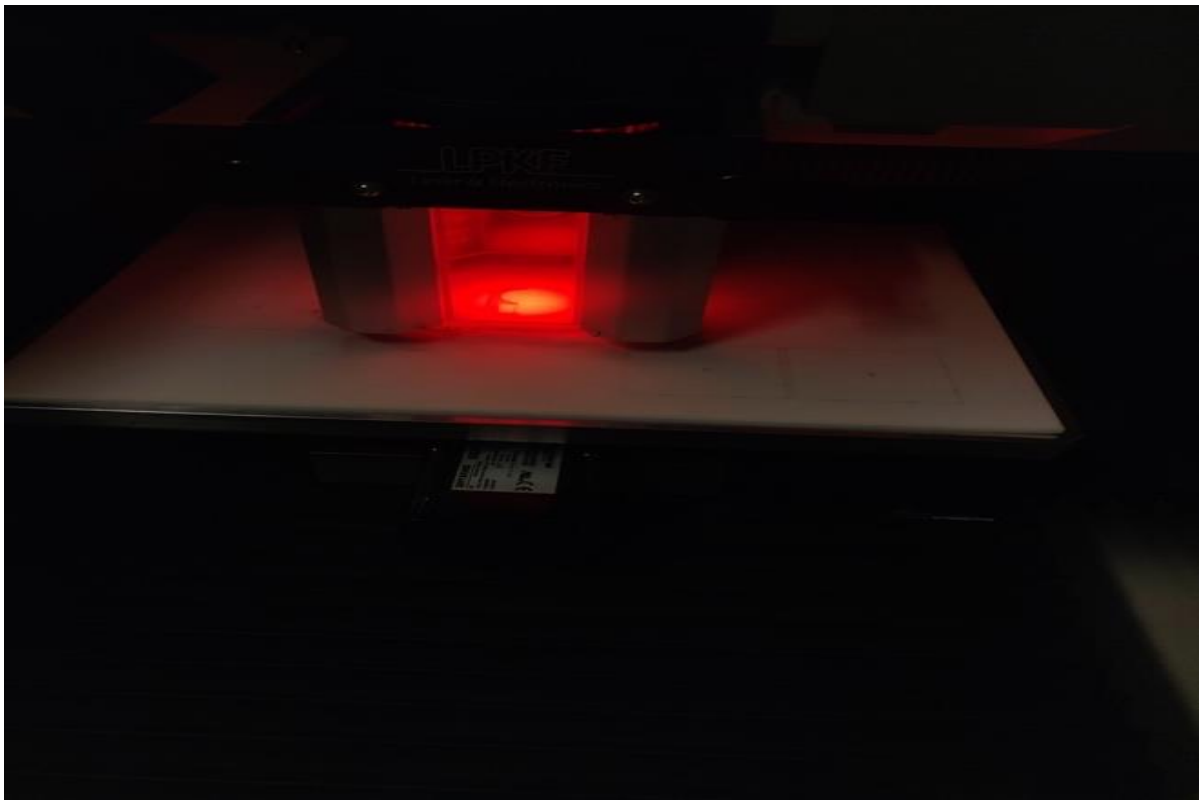

Figure 18. Antenna 2 fabrication process on LPKF ProtoLaser U3 machine using laser etching

Once the ink is applied, the Kapton substrate with the printed pattern undergoes a drying process. The purpose of drying is to remove solvents present in the ink and facilitate ink curing. In this fabrication process, the Kapton pattern is dried at 80 degrees Celsius for 60 minutes. This controlled drying period ensures that the ink adheres properly to the substrate and forms a solid, durable pattern. The next crucial step in the process is the laser etching of the antenna pattern. This is achieved using the LPKF ProtoLaser U3, a highly precise and accurate machine specifically designed for creating intricate patterns

Figure 18. The laser etching machine selectively removes the silver ink from the areas where the antenna pattern is desired. The laser beam effectively vaporizes or ablates the ink, leaving behind the desired antenna design on the Kapton substrate.

It is important to note that the accuracy and precision of the laser etching process are crucial in achieving the desired antenna performance. The LPKF ProtoLaser U3 is known for its capability to create intricate and finely detailed patterns, ensuring the reliability and efficiency of the fabricated antenna [55].

Once the laser etching process is complete, the fabricated antenna pattern may undergo further post-processing steps. These steps may include cleaning the substrate to remove any residues or contaminants that could affect the performance of the antenna. Additionally, the pattern may be inspected for any defects or imperfections, ensuring the overall quality of the fabricated antenna.

The use of these three antennas provides a comprehensive approach to tumor detection within the vest. Antenna1 and Antenna2 share the same design and characteristics, allowing for consistent performance and seamless integration into the vest material. Antenna3, with its larger radiator, enhances radiation characteristics for improved tumor detection capabilities. This

combination of antennas ensures accurate and reliable tumor detection in various breast conditions, contributing to the effectiveness of the tumor detection vest.

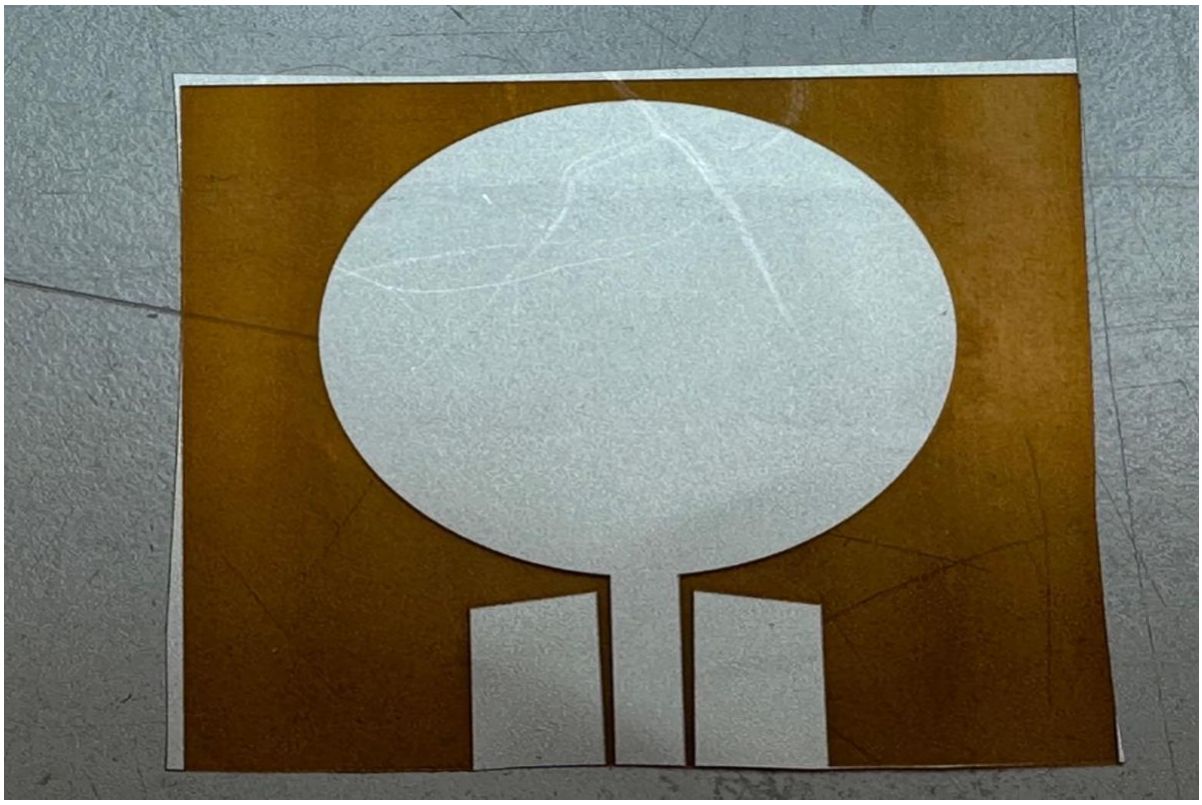

Figure 19. UWB monopole antenna with 50 um Kapton polyamide substrate (Antenna 3)

5.1.4 S11 Parameter Measurement and Comparison: Antenna 1 vs Antenna 2

Figure 20 illustrates the measurement and comparison of the S11 parameter for the PCB antenna in two different scenarios: in free space and when placed on the skin. The S11 parameter is a key indicator of antenna performance and helps assess the level of signal reflection and power transfer.

In the first scenario, the antenna is placed in free space, away from any external influences. Here, a low S11 value is observed, indicating that the antenna is well-matched to its feeding network. This means that there is minimal signal reflection, and most of the transmitted power is effectively radiated into space.

In the second scenario, the antenna is placed on the skin, which introduces a different environment and potential challenges. As a result, the S11 value increases, indicating a higher level of signal reflection. This can be attributed to impedance mismatch or interference caused by the interaction between the antenna and the skin.

The disparity in S11 values between the two scenarios highlights the impact of the skin on the antenna's performance. By comparing these measurements, we can better understand the behaviour of the antenna when in contact with the skin and evaluate the potential loss of power due to signal reflection.

Analysing the S11 parameter in different scenarios provides valuable insights for antenna design and optimization. It helps ensure efficient power transfer, minimize signal loss, and

optimize wireless communication in applications involving skin-contact devices or wearable technologies.

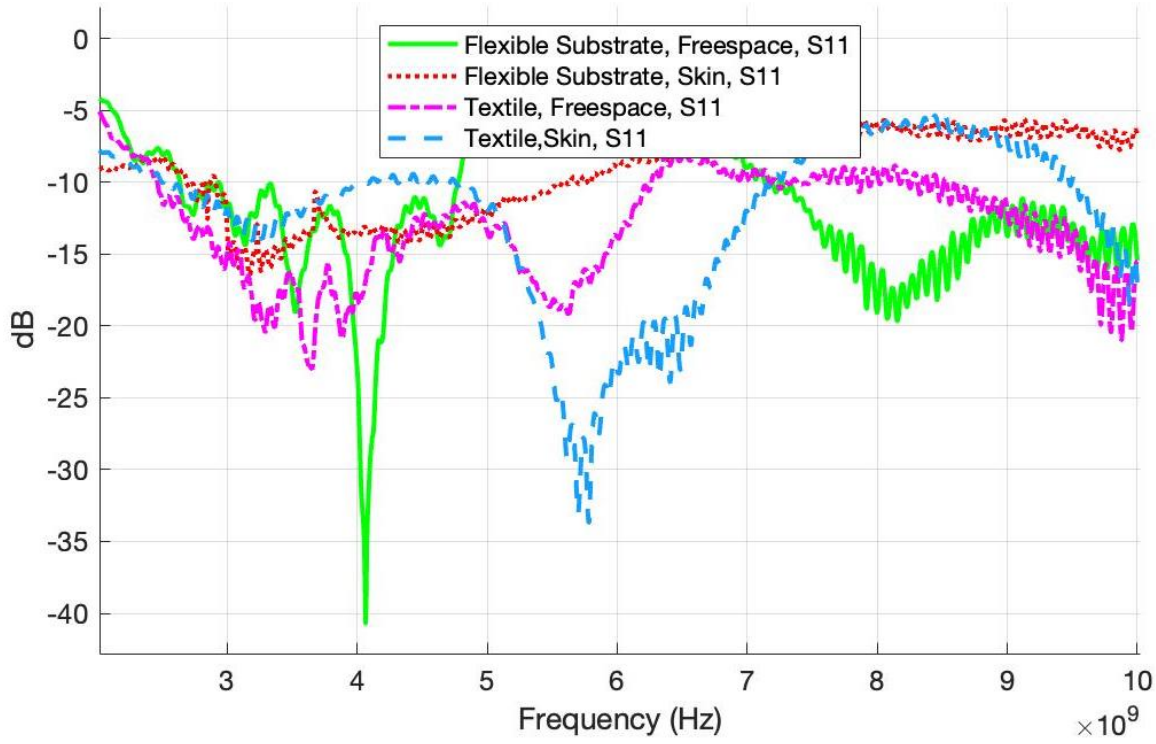

Figure 20. S11-results for 2-10 GHz bandwidth measured in freespace and on skin for Antenna 1 and Antenna 2

5.2 Vest Versions

The development of the vests involved careful consideration of the design and construction to ensure optimal performance of the antennas. In Figure 21, the first vest is depicted, featuring 8 pockets specifically tailored to accommodate the smaller monopole antennas, including both the flexible laminate and textile versions, Antennas 1 and Antenna 2 respectively. These pockets were strategically arranged based on simulations conducted in previous research [5] to achieve the best possible antenna placement for effective breast tumor monitoring.

The second vest, as shown in Figure 22, was designed with 6 pockets to accommodate the larger Kapton-based antennas. The positioning of the pockets within the vest was crucial to ensure adequate spacing between the antennas for optimal signal reception and transmission. The antennas within the same row were positioned 1.5 cm apart horizontally, while antennas in different rows were spaced 2 cm apart vertically. This arrangement allowed for sufficient isolation and minimized interference between adjacent antennas, resulting in accurate and reliable measurements.

To establish a robust connection between the antennas and the measurement equipment, SMA straight plug RF cables were employed. Specifically, P/N:415-0070-MM500 Johnson - Cinch Connectivity cables with SMA connectors on both ends were used. The flexible antennas were directly soldered to the cut side of these cables, ensuring a secure and stable connection.

The choice of RG-178 cable with an impedance of 50 ohms further guaranteed proper signal transmission and minimized signal degradation.

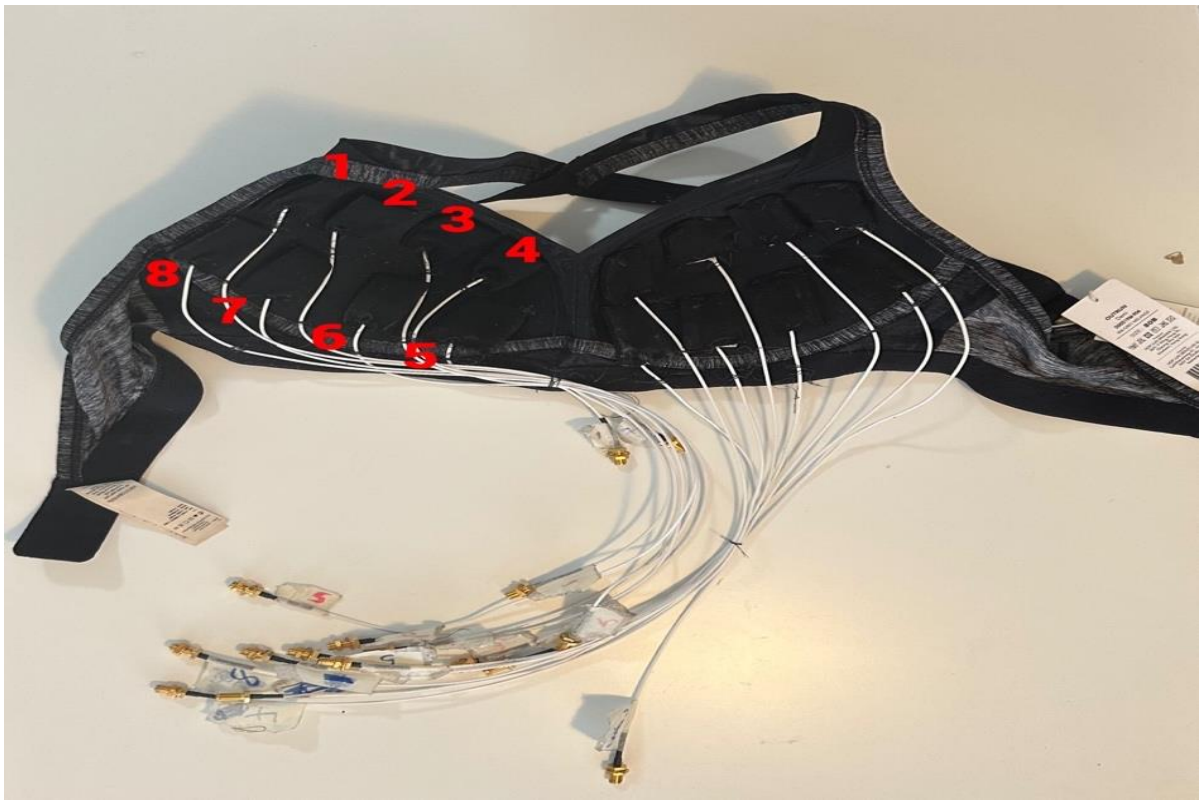

Figure 21. 8 pocket vest with 8 flexible laminate substrate antennas on LHS cup and conductive textile antennas on RHS cup

To maintain stability and minimize mechanical vibrations that could potentially affect the antenna performance, the openings of the pockets were carefully stitched. This stitching technique securely fixed the antennas within their respective pockets, preventing any unintended movement or displacement during measurements. This meticulous construction ensured that the antennas remained in their designated positions, maintaining the integrity of the measurement setup, and allowing for accurate and consistent results.

To assess the impact of the vest on the antenna's performance, the S11 parameter was measured for each antenna before and after integration into the vest. The S11 parameter, which represents the reflection coefficient, provides valuable information about how the antenna interacts with its surroundings. By comparing the S11 values before and after vest integration, the study was able to evaluate any changes in antenna characteristics caused by the vest. This comprehensive measurement approach allowed for a thorough analysis of the vest's effect on antenna performance and ensured the reliability of the obtained results.

By meticulously designing and implementing these arrangements, including the stitching of each pocket and secure attachment of the antennas to the cables, the study aimed to create a robust measurement setup for accurate assessment of the antenna's performance within the vest. These careful considerations and measurement procedures not only ensured the stability of the antenna positions but also facilitated the precise evaluation of the antennas' effectiveness in real-world breast tumor monitoring scenarios.

Overall, the detailed design of the vests, the strategic placement of antennas, and the rigorous measurement procedures all contributed to the development of a reliable system for evaluating the performance of flexible UWB antennas for breast tumor monitoring. This research aimed to advance the understanding of antenna characteristics and their integration into wearable devices, ultimately leading to the development of more effective breast tumor detection systems.

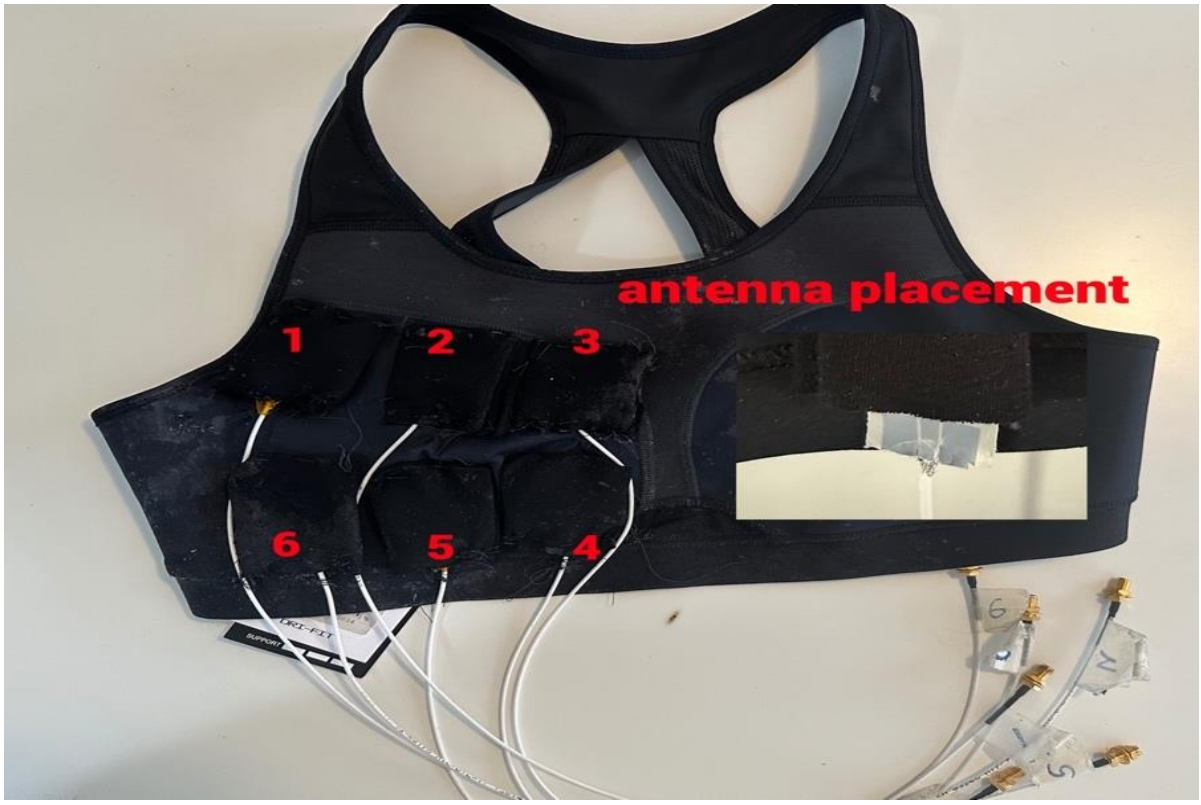

Figure 22. 6 pocket vest with kapton antennas on LHS, direction of placement of antenna shown on RHS

6 RESULTS OF VEST MEASUREMENT WITH BREAST PHANTOMS

The study investigated three different situations: a reference scenario without tumors, a scenario with a 1cm tumor, and a scenario with a 2cm tumor. The aim was to examine how the presence of tumors affects channel characteristics. To analyze this, the we measured and compared signal attenuation between selected antenna pairs for each tumor size with 2 different vests and 2 phantom types.

6.1 Vest 1 with Antenna 1, Class IV Breast Phantom

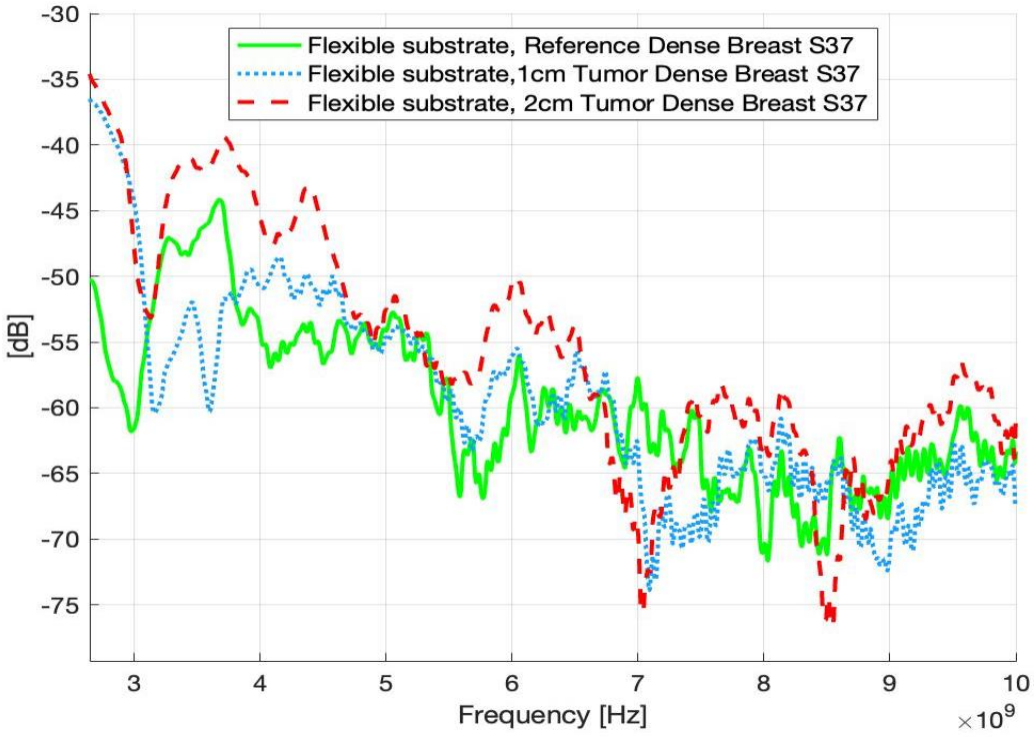

Figure 23. Channel evaluations between the antennas 3 and 7 for vests with Antenna1 and breast class IV

To evaluate the channel parameters for breast tumor monitoring, experiments were conducted using a class IV breast phantom and Vest I. The antenna used in these experiments was Antenna1, which is designed with a flexible laminate substrate. The focus of the analysis was to examine the channel characteristics between antennas 3 and 7, as well as antennas 2 and 5. These specific antenna pairs were chosen to provide insights into the effects of tumors on the channel attenuation.

From the results for antennas 3 and 7 as depicted in Figure 23, it is found that the presence of tumors decreases the channel attenuation with this selected antenna combination at most of the lower as well as higher frequencies within the measured frequency range. The difference between the 1cm tumor and reference case, is approximately 3.5 dB at 4 GHz and 5.3 dB at 8 GHz. Also, the difference between the 2cm tumor and reference case, is approximately 8.7 dB at 4 GHz and 8 dB at 8 GHz. The reason for the decrease in the channel strength is that the dielectric properties of tumor are higher than those of the glandular tissue. Thus, additional

reflections and diffraction occur for the signals which face the tumor tissue when propagating inside the breast tissue. At most of the frequencies at this range and with this antenna combination, additional reflections are summed up positively with the multipath components arriving to the receiving antenna through or on the breast tissue. The larger the tumor, the larger is the impact. Similar tendency was found in the simulation-based study presented in [1].

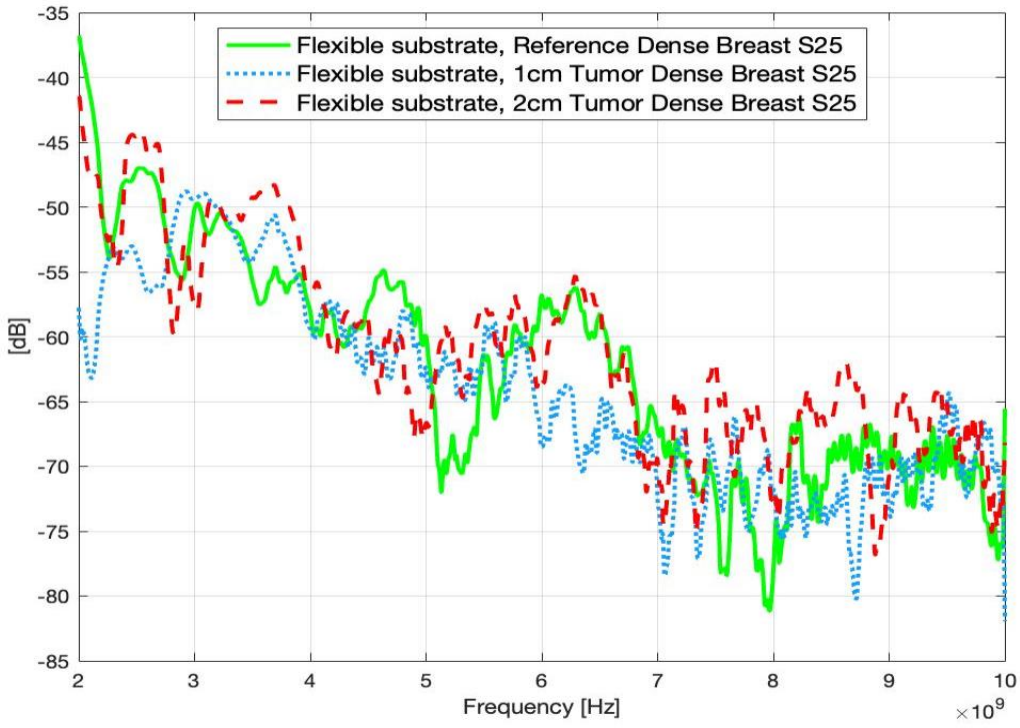

Figure 24. Channel evaluations between the antennas 2 and 5 for vests with Antenna1 and breast phantom class IV

In the case of antennas 2 and 5 in Figure 24, we observed that, the difference between 1cm tumor and reference case, is approximately -1.5 dB at 4 GHz and 7 dB at 8 GHz. For 2cm tumor case, the difference is approximately 2.3 dB at 4 GHz and 7 dB at 8 GHz. The analysis of the channel parameters consistently showed a decrease in channel attenuation when tumors were present, regardless of the specific antenna combination.

6.2 Vest 1 with Antenna 1, Class II Breast Phantom

Experiments using a class II breast phantom and Antenna1 revealed that the presence of tumors decreased channel attenuation between antennas 3 and 7 at higher frequencies as well as lower frequencies. The difference between the 1cm tumor and reference case, is approximately 4 dB at 4 GHz and 1.7 dB at 8 GHz. Also, the difference between the 2 cm tumor and reference case, is approximately 5.2 dB at 4 GHz and 1 dB at 8 GHz which can be seen from Figure 25.

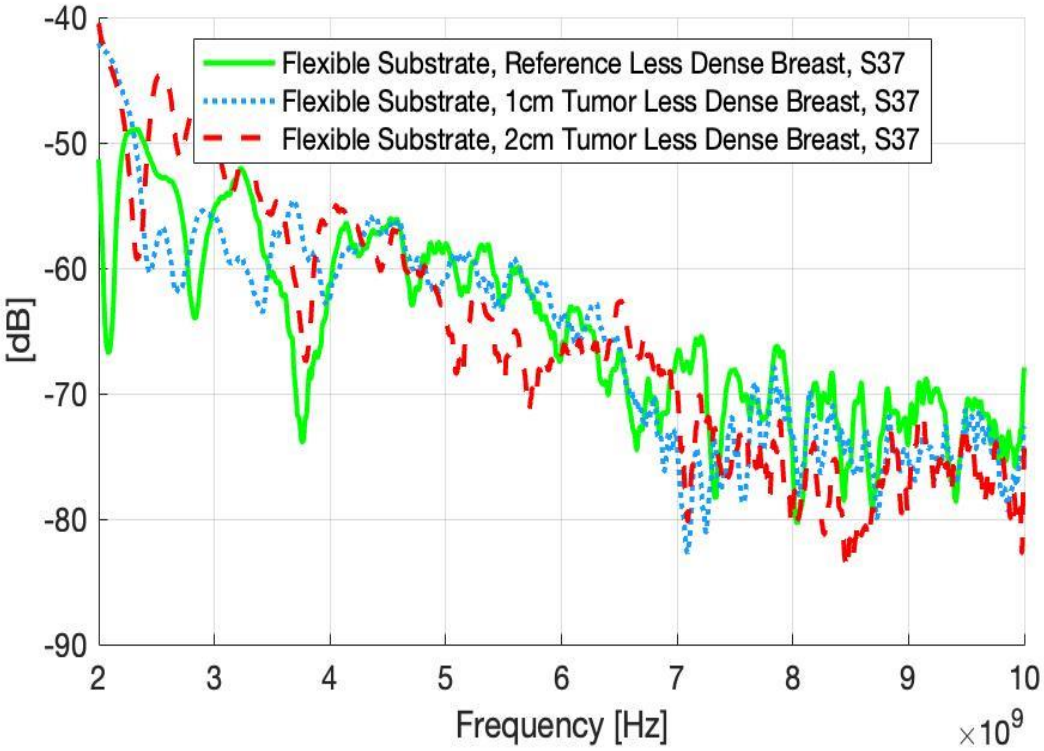

Figure 25. Channel evaluations between the antennas 3 and 7 for vests with Antenna1 and breast class II

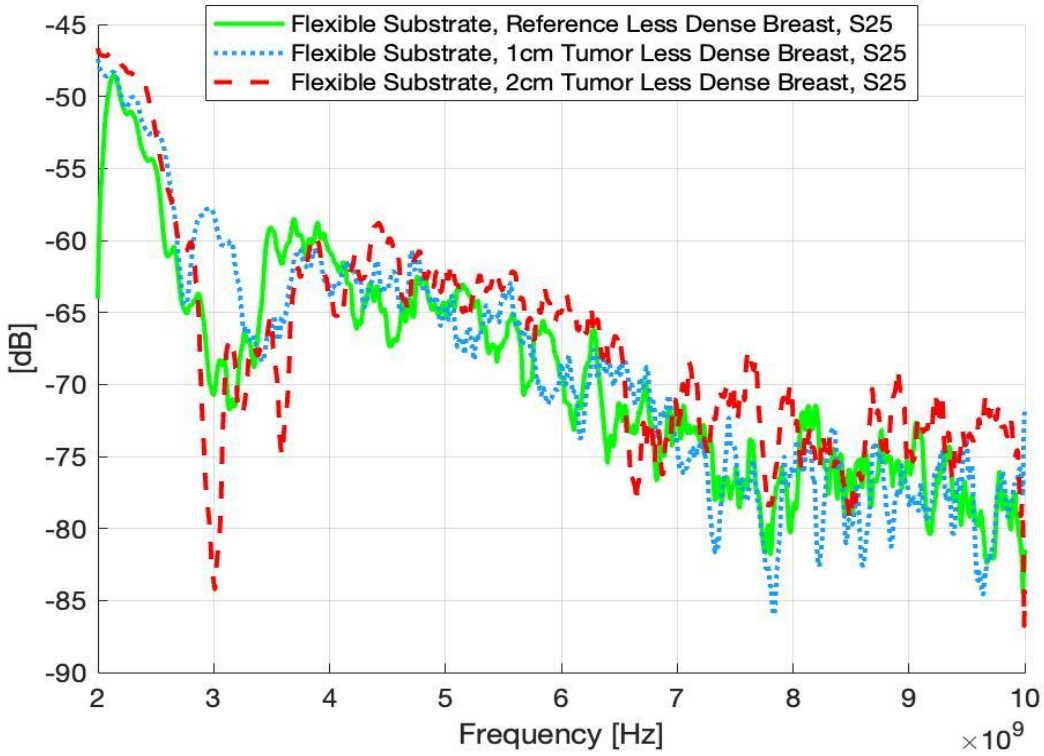

Figure 26. Channel evaluations between the antennas 2 and 5 for vests with Antenna1 and breast class II

In the case of antennas 2 and 5 in Figure 26, we observed that the presence of tumors decreased channel attenuation at only higher frequencies, the difference between 1cm tumor and reference case, is approximately -2.46 dB at 4 GHz and 2.65 dB at 8 GHz. For 2cm tumor case, the difference is approximately -3.28 dB at 4 GHz and 6.35 dB at 8 GHz. It is seen that, the analysis of the channel parameters consistently showed a decrease in channel attenuation when tumors were present, regardless of the specific antenna combination at higher frequency of 8 GHz.

In less dense breast tissue (breast class II), the differences in channel parameters caused by tumors are slightly smaller compared to denser breast types. This is because fat, which is a less obstructive medium, allows the strongest signal components to primarily come from fat propagation. Although the changes induced by tumors are less pronounced, they are still detectable. This suggests that tumor detection is possible even in less dense breast tissues.

6.3 Vest 1 with Antenna 2, Class IV Breast Phantom

Experimental investigations using a class IV breast phantom and Antenna 2 demonstrated that the presence of tumors had a significant impact on channel attenuation between specific antennas and at different frequencies. Between antennas 3 and 7 in Figure 27, it was observed that the channel attenuation decreased at both higher and lower frequencies in the presence of tumors, compared to the reference case. The difference in attenuation between the 1cm tumor and reference case was approximately 4 dB at 4 GHz and 3 dB at 8 GHz. Similarly, the difference between the 2 cm tumor and reference case was approximately 7.2 dB at 4 GHz and 2 dB at 8 GHz.

For antennas 2 and 5 in Figure 28, the presence of tumors also resulted in a decrease in channel attenuation. In the case of the 2cm tumor, this decrease was observed at both higher and lower frequencies, while for the 1 cm tumor, it was observed only at lower frequencies. Specifically, the difference in attenuation between the 1cm tumor and reference case was approximately 13.6 dB at 4 GHz and -6.5 dB at 8 GHz. For the 2cm tumor case, the difference was approximately 21 dB at 4 GHz and 6 dB at 8 GHz. These findings highlight the significant impact of tumor presence on channel characteristics and provide valuable insights for breast tumor monitoring using microwave imaging systems.

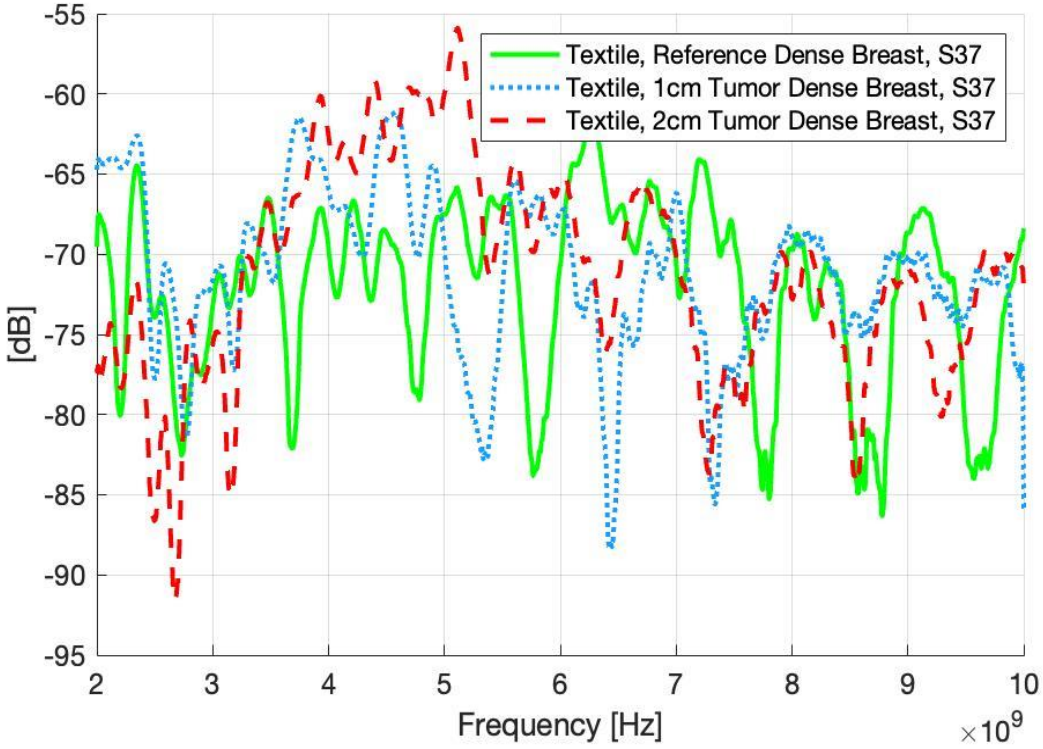

Figure 27. Channel evaluations between the antennas 3 and 7 for vests with Antenna2 and breast class IV

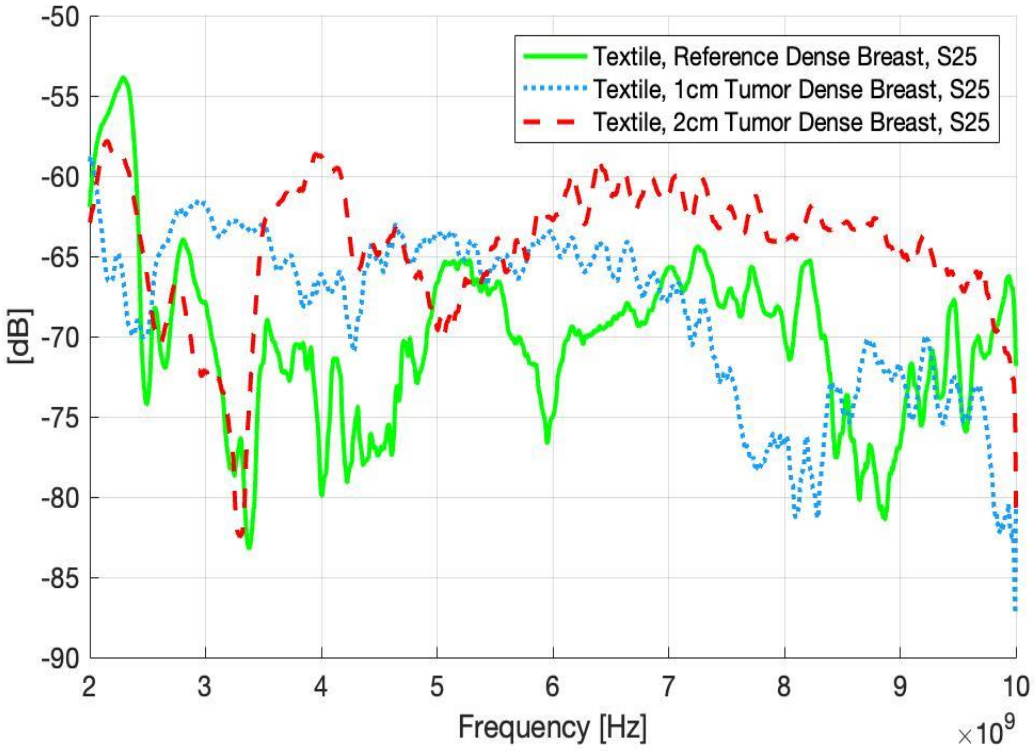

Figure 28. Channel evaluations between the antennas 2 and 5 for vests with Antenna2 and breast class IV

6.4 Vest 1 with Antenna 2, Class II Breast Phantom

The evaluation was further extended to include the use of Vest I with a conductive textile antenna configuration, providing an alternative setup for channel parameter assessments. Experimental investigations using a class II breast phantom and Antenna 2 revealed significant effects of tumor presence on channel attenuation between specific antennas and across different frequencies. Between antennas 3 and 7 in Figure 29, the presence of tumors resulted in decreased channel attenuation more prominently at higher frequencies, compared to the reference case. The difference in attenuation between the 1cm tumor and reference case was approximately -5 dB at 4 GHz and 6 dB at 8 GHz. Similarly, the difference between the 2 cm tumor and reference case was approximately 12 dB at 4 GHz and 14 dB at 8 GHz.

For antennas 2 and 5 in Figure 30, the presence of tumors also led to a decrease in channel attenuation. The decrease in channel attenuation was observed primarily at lower frequencies. Specifically, the difference in attenuation between the 1cm tumor and reference case was approximately 4 dB at 4 GHz and 0.5 dB at 8 GHz. For the 2cm tumor case, the difference was approximately 1.8 dB at 4 GHz and 0.6 dB at 8 GHz. These findings highlight the significant impact of tumors on channel characteristics, demonstrating the potential of the Vest I setup with textile antenna for breast tumor monitoring using microwave imaging systems.

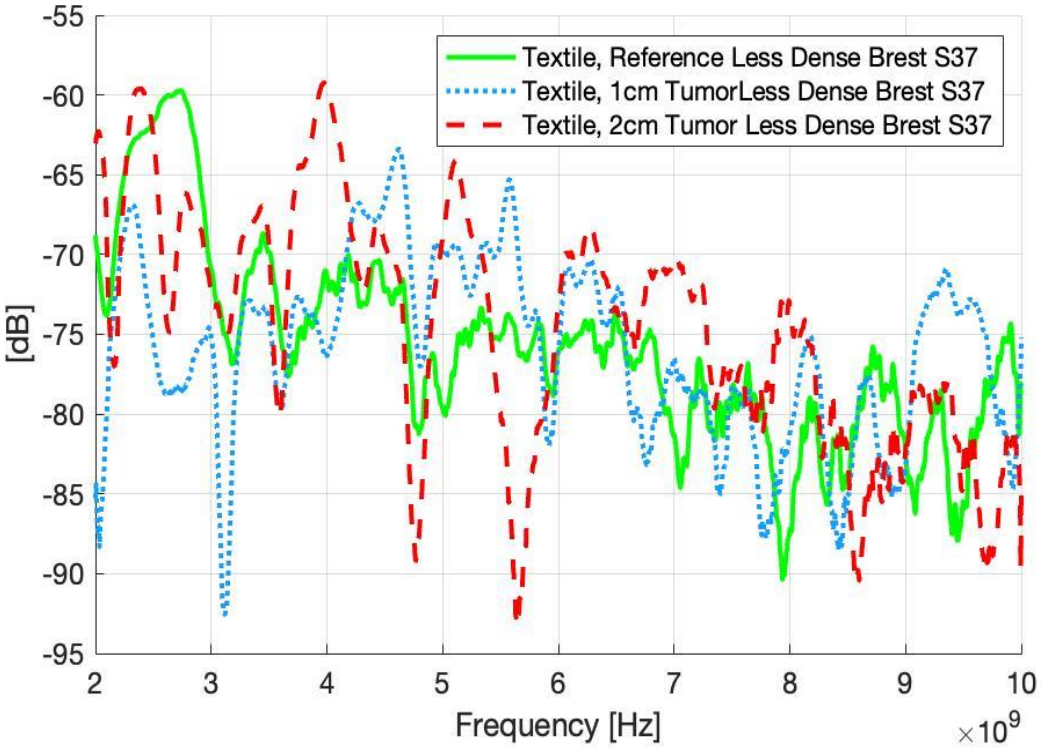

Figure 29. Channel evaluations between the antennas 3 and 7 for vests with Antenna2 and breast class II

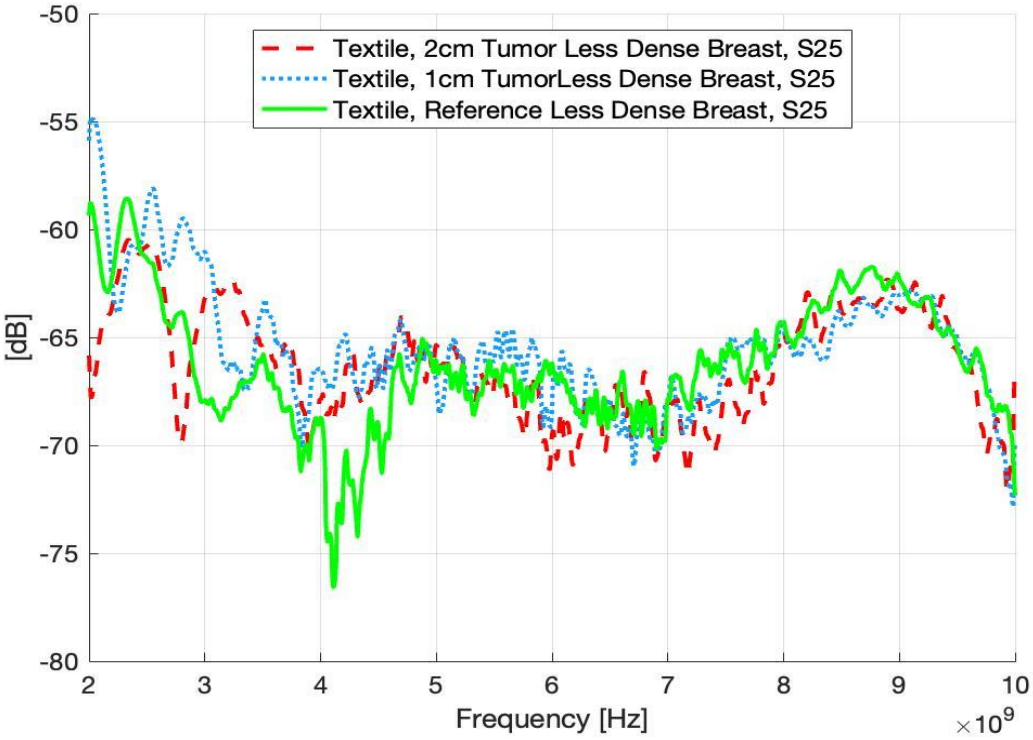

Figure 30. Channel evaluations between the antennas 2 and 5 for vests with Antenna2 and breast class II

6.5 Vest 2 with Antenna 3, Class IV Breast Phantom

The study also examined the performance of Vest II, a system designed for larger breast phantoms. Channel parameter evaluations for breast tumor monitoring were carried out using a class IV breast phantom. The experiments utilized Antenna 3, which is the bigger antenna (monopole 2) constructed with a flexible Kapton polyamide substrate. The primary objective was to analyze the channel characteristics between antennas 1 and 5, to understand the influence of tumors on channel attenuation.

The difference between the 1cm tumor and reference case illustrated in Figure 31, is approximately 5 dB at 4 GHz and 18.5 dB at 8 GHz. Also, the difference between the 2 cm tumor and reference case, is approximately 2.15 dB at 4 GHz and 14.8 dB at 8 GHz.

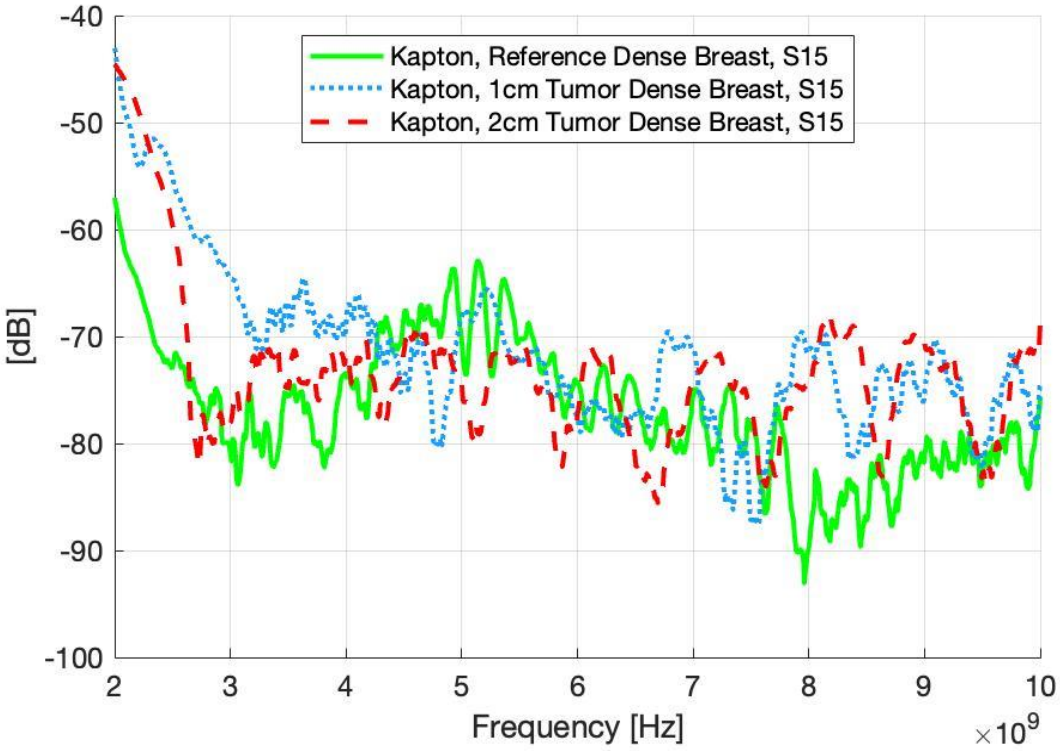

Figure 31. Channel evaluations between the antennas 1 and 5 for vest 2 with Antenna3 and breast class IV

6.6 Vest 2 with Antenna 3, Class II Breast Phantom

In addition to the previous findings, the study further included the assessment of channel parameters for a class II breast phantom using Antenna 3. The channel characteristics between antennas 1 and 5 were investigated for this less dense breast depicted in Figure 32. The difference between the 1cm tumor and reference case, is approximately 3 dB at 4 GHz and 0.5 dB at 8 GHz. Also, the difference between the 2 cm tumor and reference case, is approximately 1.4 dB at 4 GHz and 9 dB at 8 GHz.

Overall, with Vest II, the differences caused by tumors are more prominent, particularly in breast class IV. The results revealed that the effects of tumors on channel parameters remained distinguishable, even with larger breast phantoms. This observation indicates that the Vest II setup is reliable and effective in detecting tumors across different breast sizes. The findings highlight the consistent ability of the Vest II system to identify and detect tumors based on changes in channel characteristics.

The analysis of channel parameters consistently demonstrated a decrease in channel attenuation when tumors were present, indicating higher dielectric properties of tumor tissue compared to glandular tissue. This decrease ranged from 0.5 to 21 dB, depending on frequency and tumor size. Tumors introduce additional reflections and diffraction, significantly affecting signal propagation within the breast tissue. Various factors, including tumor size, breast density, and antenna configuration, influence the observed changes in channel characteristics. These findings highlight the detectability of tumors and provide insights for developing effective tumor detection systems. Understanding tumor effects on channel parameters and considering breast tissue characteristics can advance the design of breast tumor monitoring technologies,

contributing to early detection, improved patient outcomes, and advancements in breast cancer research.

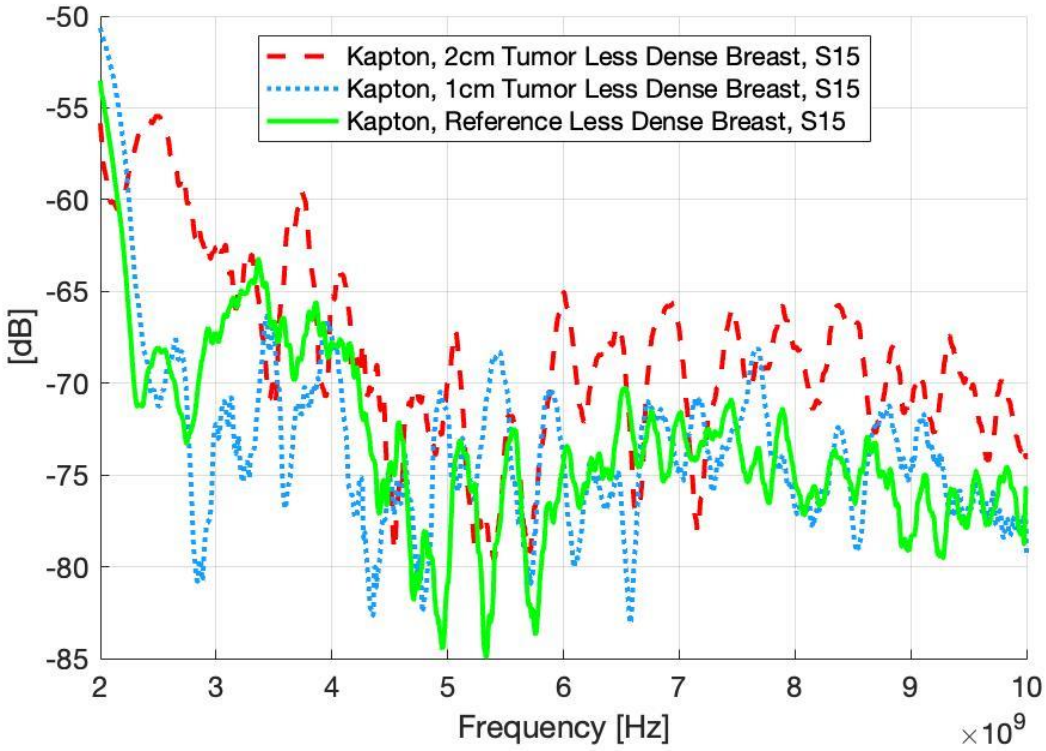

Figure 32. Channel evaluations between the antennas 1 and 5 for vest 2 with Antenna3 and breast class II

7 DISCUSSION

The findings and implications of this study provide valuable insights into the field of breast tumor monitoring and detection. The development of a prototype breast tumor monitoring vest using UWB flexible antennas has shown promising potential for enhancing the early detection of breast tumors. By leveraging the unique characteristics of radio channels among multiple on-body antennas embedded in the vest, even small tumors as small as 1cm can be detected, leading to improved diagnostic outcomes and more effective treatment interventions.

One notable finding of this study is the effectiveness of higher frequencies, specifically in the range of 7-8 GHz, for breast tumor detection. These frequencies have demonstrated superior resolution and a substantial contrast in relative permittivity between tumor tissue and breast glandular tissue. This enhanced contrast enables the accurate identification and localization of tumors, which is essential for timely diagnosis and targeted treatment planning. The utilization of higher frequencies in breast tumor detection represents a significant advancement in the field, as it provides a more detailed understanding of tumor characteristics and improves the accuracy of diagnostic measurements.

The successful development of novel tissue phantoms played a vital role in this research. The careful selection of ingredients and the formulation development process resulted in tissue phantoms that closely mimic the dielectric properties of human tissues [57]. These phantoms served as reliable and reproducible replicas, providing a platform for evaluating the performance and effectiveness of the breast tumor monitoring vest. By accurately simulating the electromagnetic properties of human tissues, the tissue phantoms enable researchers to conduct rigorous experiments and investigations, ultimately contributing to the advancement of breast imaging technology.

Looking ahead, the integration of advanced AI algorithms presents a promising avenue for enhancing the diagnostic capabilities of the monitoring vest. By incorporating AI-based channel analysis, the vest can further improve the accuracy and reliability of tumor detection, potentially reducing false positives and enabling real-time monitoring of breast health. This integration holds significant potential for enhancing the clinical accuracy and efficiency of breast tumor screening, making it a valuable tool in healthcare settings, particularly in resource-limited areas and for home monitoring applications. AI algorithms can analyze complex radio channel data, identify patterns, and extract meaningful information, aiding in the early detection and monitoring of breast tumors. The ability to leverage AI algorithms in conjunction with the breast tumor monitoring vest represents a major step forward in the field of breast imaging and has the potential to significantly improve breast healthcare.

Furthermore, the utilization of mm-range frequencies in the breast tumor monitoring vest offers additional benefits beyond diagnostic measurements. These frequencies enable seamless wireless communication, paving the way for telemedicine applications and the establishment of advanced wireless hospitals. By leveraging wireless communication capabilities, medical professionals can remotely monitor patients' breast health and provide real-time consultations, leading to improved access to healthcare services and better patient outcomes. The integration of cutting-edge technologies, such as 6G, can further enhance the wireless communication capabilities of the monitoring vest, enabling faster data transmission, higher reliability, and increased scalability.

It is important to acknowledge that further studies are needed to validate the clinical accuracy and effectiveness of the proposed method across different tumor types. Additionally, considerations such as scalability, power efficiency, data transmission, and patient acceptance

should be addressed to ensure the practical implementation and widespread adoption of the monitoring vest. The research presented in this thesis lays the groundwork for future studies to explore these aspects and refine the breast tumor monitoring vest for practical clinical applications.

In conclusion, the findings of this study highlight the potential of the breast tumor monitoring vest using UWB flexible antennas as a valuable tool for breast tumor detection. The use of higher frequencies and the successful development of tissue phantoms provide a foundation for accurate tumor identification and localization. By integrating advanced AI algorithms and embracing emerging technologies, such as 6G, the diagnostic capabilities of the monitoring vest can be further enhanced. Through continued research and development, this technology has the potential to significantly impact breast healthcare by enabling early detection, improving treatment outcomes, and ultimately, enhancing patient well-being. The integration of wireless communication capabilities further extends the potential of the monitoring vest, enabling remote monitoring, telemedicine applications, and the establishment of advanced wireless hospitals. The future holds tremendous opportunities for the advancement of breast imaging technology, and the findings presented in this thesis contribute to the ongoing progress in this important field of research.

8 SUMMARY OF THESIS

The introduction provides an overview of the global significance of breast cancer as a health concern and the limitations of existing breast cancer screening methods. It introduces the concept of microwave-based breast cancer monitoring and highlights the promising findings from a previous research paper. The objective of the master thesis is presented, which is to develop and evaluate a self-monitoring vest equipped with UWB antennas and channel analysis to overcome the limitations of current screening methods and enable regular breast cancer monitoring from home.

The "Background and Literature Review," provides a comprehensive overview of the relevant topics related to microwave techniques for breast cancer detection. It starts by discussing the anatomy of the female breast, highlighting the importance of understanding its structure for effective tumor detection. The section then delves into the microwave properties of the human breast, elucidating the interactions between microwaves and breast tissue. The basic principle of microwave channel analysis is explained, emphasizing its significance in detecting breast tumors. Furthermore, the advantages of microwave-based tumor detection methods are explored, showcasing their potential for improved breast cancer screening. Various microwave techniques used in breast cancer detection, including microwave tomography and radar-based UWB microwave imaging, are discussed, along with different self-monitoring vests integrated with UWB antennas. This section serves as a foundation for the subsequent chapters of the thesis, providing a comprehensive background and literature review to support the research and development of the practical self-monitoring vest for early detection of small-sized breast tumors.

The "Preparation of Tissue Phantoms" section in the master's thesis explores the comprehensive methodology for creating tissue phantoms that replicate the dielectric properties of various human tissues. While the section primarily focuses on fat tissue, it also acknowledges the existence of other phantom types. The outlined approach involves careful ingredient selection, formulation development, fabrication techniques, and stability evaluation for the creation of skin, muscle, fat, tumor, and gland tissue phantoms. By following these procedures, researchers can successfully produce tissue phantoms that closely mimic the properties of real human tissues. These phantoms serve as essential tools for investigating microwave-based applications in medical diagnostics and provide a reliable and versatile platform for further research in the field.

The third section discusses the assembly of heterogeneous breast phantoms used for evaluating the performance of the tumor detection vest. The phantoms consisted of outer and inner molds, with the outer molds resembling the shape of a prone human breast. Two breast density types, representing very dense and less dense breasts, were used. For the dense breast phantoms, liquid fat material was solidified in the outer molds, and a glandular liquid was poured into the inner mold, with tumors inserted and covered with additional glandular liquid. For the less dense breast phantoms, fat liquid was solidified in the outer molds, and cylindrical glandular molds were inserted. A skin layer and muscle layer were added to complete the assembly, accurately simulating the composition and structure of a breast. This realistic breast phantom assembly allowed for accurate measurements and evaluation of the vest's performance under different breast density conditions, contributing to breast imaging research and development.

The "Monitoring Vest" section discusses the antennas used in the tumor detection vest and the design of two different vest versions. Antenna1 is a UWB monopole antenna with a flexible laminate substrate, while Antenna2 is a textile-based version of Antenna1. Antenna3 has a

Kapton-based substrate and larger dimensions. The combination of these antennas ensures accurate tumor detection in various breast conditions. The section also highlights the measurement and comparison of the S11 parameter for the PCB antenna in free space and when placed on the skin, emphasizing the impact of the skin on antenna performance. The section concludes by describing the design of the vests, including the arrangement of pockets and the use of RF cables for connection. The careful design and implementation of the vests and antenna placement ensure accurate measurements and reliable performance evaluation.

The results section of the study shows that the presence of tumors in breast tissue leads to a noticeable decrease in channel attenuation. The higher dielectric properties of tumors cause additional reflections and diffraction, affecting signal propagation within the breast. These changes in channel characteristics are influenced by factors such as tumor size, breast density, and antenna configuration. The study demonstrates the detectability of tumors and provides valuable insights for developing effective tumor detection systems in different breast tissue scenarios.

In this master thesis, a prototype of a breast tumor monitoring vest utilizing UWB flexible antennas was developed and evaluated. The research demonstrated the effectiveness of the vest in detecting breast tumors, even as small as 1cm, by leveraging the distinct characteristics of radio channels among multiple on-body antennas embedded in the vest. Higher frequencies in the 7-8 GHz range showed improved resolution and contrast in relative permittivity, enhancing the accuracy of tumor detection. The development of tissue phantoms played a crucial role, enabling reliable experiments to mimic human tissues. Integration of advanced AI algorithms and 6G technology holds promise for enhancing diagnostic capabilities and revolutionizing healthcare. Overall, the breast tumor monitoring vest shows potential for widespread implementation in breast health checks, home monitoring, and wireless healthcare systems.

9 REFERENCES

[1] Dessai, R., Särestöniemi, M., Myllymäki, S., Reponen, J., & Myllylä, T. (in review). Breast Tumor Monitoring Vest with Embedded Flexible UWB Antennas – The First Proof-of-Concept.IEEE International Microwave Biomedical Conference.

[2] Särestöniemi, M., Myllymäki, S., Reponen, J., & Myllylä, T. (2023). Remote diagnostics and monitoring using microwave technique – improving healthcare in rural areas and in exceptional situations. Finnish Journal of EHealth and EWelfare, 15(1), pp. 6–22.

[3] Kuwahara, Y. (2017). Microwave Imaging for Early Breast Cancer Detection. InTech. doi: 10.5772/intechopen.69562

[4] O'Loughlin, D., O'Halloran, M., Moloney, B. M., Glavin, M., Jones, E., & Elahi, M. A. (2018). Microwave Breast Imaging: Clinical Advances and Remaining Challenges. IEEE Transactions on Biomedical Engineering, 65(11), pp. 2580-2590.

[5] Särestöniemi, M., Myllymäki, S., Reponen, J., & Myllylä, T. (2023). Remote diagnostics and monitoring using microwave technique – improving healthcare in rural areas and in exceptional situations. Finnish Journal of EHealth and EWelfare, 15(1), pp. 6–22.

[6] Jafarifarmand, A., Yilmaz, T., & Akduman, I. (2022). Microwave Medical Diagnosis System with a Framework to Optimize the Antenna Configuration and Frequency of Operation Using Neural Networks. IEEE Transactions on Microwave Theory and Techniques, 70(11), pp. 5095-5104.

[7] Lu, M., Xiao, X., Pang, Y., Liu, G., & Lu, H. (2022). Detection and Localization of Breast Cancer Using UWB Microwave Technology and CNN-LSTM Framework. IEEE Transactions on Microwave Theory and Techniques, 70(11), pp. 5085-5094.

[8] Bahramiabarghouei, H., Porter, E., Santorelli, A., Gosselin, B., Popović, M., & Rusch, L. A. (2015). Flexible 16 Antenna Array for Microwave Breast Cancer Detection. IEEE Transactions on Biomedical Engineering, 62(10), 2516-2525.

[9] Neira, L. M., Mays, R. O., & Hagness, S. C. (2017). Human Breast Phantoms: Test Beds for the Development of Microwave Diagnostic and Therapeutic Technologies. IEEE Pulse, 8(4), pp. 66-70.

[10] Costanzo, S., Cioffi, V., Qureshi, A. M., & Borgia, A. (2021). Gel-Like Human Mimicking Phantoms: Realization Procedure, Dielectric Characterization and Experimental Validations on Microwave Wearable Body Sensors. Biosensors, 11(4), 111 p.

[11] Garrett, J., & Fear, E. (2014). Stable and Flexible Materials to Mimic the Dielectric Properties of Human Soft Tissues. IEEE Antennas and Wireless Propagation Letters, 13, pp. 599-602.

[12] Castelló-Palacios, S., Garcia-Pardo, C., Fornes-Leal, A., Cardona, N., & Vallés-Lluch, A. (2016). Tailor-Made Tissue Phantoms Based on Acetonitrile Solutions for Microwave Applications up to 18 GHz. IEEE Transactions on Microwave Theory and Techniques, 64(11), pp. 3987-3994.

[13] Pollacco, D. A., Conti, M. C., Farrugia, L., Wismayer, P. S., Farina, L., & Sammut, C. V. (2019). Dielectric properties of muscle and adipose tissue-mimicking solutions for microwave medical imaging applications. Physics in medicine and biology, 64(9), 095009.

[14] Di Meo, S., Pasotti, L., Iliopoulos, I., Pasian, M., Ettorre, M., Zhadobov, M., & Matrone, G. (2019). Tissue-mimicking materials for breast phantoms up to 50 GHz. Physics in medicine and biology, 64(5), 055006.

[15] Lazebnik, M., Madsen, E. L., Frank, G. R., & Hagness, S. C. (2005). Tissue-mimicking phantom materials for narrowband and ultrawideband microwave applications. Physics in medicine and biology, 50(18), pp. 4245–4258.

[16] Porter, E., Fakhoury, J., Oprisor, R., Coates, M., & Popović, M. (2010). Improved tissue phantoms for experimental validation of microwave breast cancer detection. In Proceedings of the Fourth European Conference on Antennas and Propagation, Barcelona, Spain, pp. 1-5.

[17] Martellosio, A., et al. (2017). Dielectric Properties Characterization From 0.5 to 50 GHz of Breast Cancer Tissues. IEEE Transactions on Microwave Theory and Techniques, 65(3), pp. 998-1011.

[18] Meo, S. D., et al. (2019). Tissue mimicking materials for breast phantoms using waste oil hardeners. In 2019 13th European Conference on Antennas and Propagation (EuCAP), Krakow, Poland, pp. 1-4.

[19] Rydholm, T. (2018). Experimental Evaluation of a Microwave Tomography System for Breast Cancer Detection.

[20] Gabriel, C., Gabriel, S., & Corthout, Y. E. (1996). The dielectric properties of biological tissues: I. Literature survey. Physics in medicine & biology, 41(11), 2231p.

[21] Lazebnik, M., Popovic, D., McCartney, L., Watkins, C. B., Lindstrom, M. J., Harter, J., & Hagness, S. C. (2007). A large-scale study of the ultrawideband microwave dielectric properties of normal, benign, and malignant breast tissues obtained from cancer surgeries. Physics in medicine & biology, 52(20), 6093.

[22] Fear, E. C., Meaney, P. M., & Stuchly, M. A. (2003). Microwaves for breast cancer detection? IEEE Potentials, 22(1), 12-18. doi: 10.1109/MP.2003.1180933.

[23] Kwon, S., & Lee, S. (2016). Recent Advances in Microwave Imaging for Breast Cancer Detection. International journal of biomedical imaging, 2016, 5054912.

[24] Meaney, P. M., Golnabi, A. H., Epstein, N. R., Geimer, S. D., Fanning, M. W., Weaver, J. B., & Paulsen, K. D. (2013). Integration of microwave tomography with magnetic resonance for improved breast imaging. Medical physics, 40(10), 103101.

[25] Meaney, P. M., Fanning, M. W., Zhou, T., Golnabi, A., Geimer, S. D., & Paulsen, K. D. (2009). Clinical microwave breast imaging—2D results and the evolution to 3D. In Proceedings of the 2009 International Conference on Electromagnetics in Advanced Applications (ICEAA'09), Torino, Italy, pp. 881-884.

[26] Grzegorczyk, T. M., Meaney, P. M., Kaufman, P. A., Diforio-Alexander, R. M., & Paulsen, K. D. (2012). Fast 3-D tomographic microwave imaging for breast cancer detection. IEEE Transactions on Medical Imaging, 31(8), pp.1584-1592.

[27] Son, S.-H., Simonov, N., Kim, H.-J., Lee, J.-M., & Jeon, S.-I. (2010). Preclinical Prototype Development of a Microwave Tomography System for Breast Cancer Detection. ETRI Journal, 32, 901-910.

[28] Amineh, R. K., Ravan, M., Trehan, A., & Nikolova, N. K. (2011). Near-Field Microwave Imaging Based on Aperture Raster Scanning with TEM Horn Antennas. IEEE Transactions on Antennas and Propagation, 59(3), 928-940.

[29] Flores-Tapia, D., Maizlish, O., Alabaster, C., & Pistorius, S. (2012, May). Microwave radar imaging of inhomogeneous breast phantoms using circular holography. In 2012 9th IEEE International Symposium on Biomedical Imaging (ISBI) (pp. 86-89). IEEE.

[30] Mohammed, B. A. J., Abbosh, A. M., & Sharpe, P. (2013). Planar array of corrugated tapered slot antennas for ultrawideband biomedical microwave imaging system. International Journal of RF and Microwave Computer-Aided Engineering, 23(1), pp. 59-66.

[31] Klemm, M., Craddock, I. J., Leendertz, J. A., Preece, A., & Benjamin, R. (2009). Radar-based breast cancer detection using a hemispherical antenna array - Experimental results. IEEE Transactions on Antennas and Propagation, 57(6), pp. 1692-1704.

[32] L. Fortaleza, L. Kranold, and M. Popović. (2020). Flexible 16-Antenna System for Microwave Breast Screening: NB vs. UWB Performance. In 2020 IEEE International Symposium on Antennas and Propagation and North American Radio Science Meeting, pp. 1289-1290.

[33] W. Kendall, L. Kranold, C. Hahn, S. Studebaker, J. Schwartz, and M. Popović. (2020). A Flexible Antenna Array with Integrated Switching Matrix for Breast Cancer Detection. In 2020 42nd Annual International Conference of the IEEE Engineering in Medicine & Biology Society (EMBC), pp. 4369-4372.

[34] M. M. U. Rashid, A. Rahman, L. C. Paul, J. Rafa, B. Podder, and A. K. Sarkar. (2019). Breast Cancer Detection & Tumor Localization Using Four Flexible Microstrip Patch Antennas. In 2019 International Conference on Computer, Communication, Chemical, Materials, and Electronic Engineering (IC4ME2), pp. 1-6.

[35] Särestöniemi, M., Sonkki, M., Myllymäki, S., & Pomalaza-Raez, C. (2021). Wearable Flexible Antenna for UWB On-Body and Implant Communications. Telecom, 2(3), pp. 285-301.

[36] H. Bahrami, E. Porter, A. Santorelli, B. Gosselin, M. Popovic, and L. A. Rusch. (2014). Flexible sixteen monopole antenna array for microwave breast cancer detection. In 2014 36th Annual International Conference of the IEEE Engineering in Medicine and Biology Society, pp. 3775-3778.

[37] Rahman, A., Islam, M. T., Singh, M. J., Kibria, S., & Akhtaruzzaman, M. (2016). Electromagnetic Performances Analysis of an Ultra-wideband and Flexible Material Antenna in Microwave Breast Imaging: To Implement a Wearable Medical Bra. Scientific reports, 6, 38906.

[38] Wang, F., Arslan, T., & Wang, G. (2017). Breast cancer detection with microwave imaging system using wearable conformal antenna arrays. 2017 IEEE International Conference on Imaging Systems and Techniques (IST), pp. 1-6.

[39] Elsheakh, D. M., Alsherif, S. A., & Eldamak, A. R. (2023). Textile monopole sensors for breast cancer detection. Telecommunication Systems, 82, pp.363-379.

[40] Mahmood, S. N., Ishak, A. J., Jalal, A., Saeidi, T., Shafie, S., Soh, A. C., Imran, M. A., & Abbasi, Q. H. (2021). A Bra Monitoring System Using a Miniaturized Wearable Ultra-Wideband MIMO Antenna for Breast Cancer Imaging. Electronics, 10(21), 2563 p.

[41] Elsheakh, D. N., Elgendy, Y. K., Elsayed, M. E., & Eldamak, A. R. (2023). Circularly Polarized Textile Sensors for Microwave-Based Smart Bra Monitoring System. Micromachines, 14(3), 586 p.

[42] Borja, B., Tirado-Méndez, J. A., & Jardon-Aguilar, H. (2018). An overview of UWB antennas for microwave imaging systems for cancer detection purposes. Progress In Electromagnetics Research B, 80, pp. 173-198.

[43] Ray, P. P., Dash, D., & De, D. (2017). A Systematic Review of Wearable Systems for Cancer Detection: Current State and Challenges. Journal of Medical Systems, 41, 180 p.

[44] Canicattì, E., et al. (2022). Anatomical and Dielectric Tissue Mimicking Phantoms for Microwave Breast Imaging. 2022 16th European Conference on Antennas and Propagation (EuCAP), pp. 1-4.

[45] Rana, S. P., Dey, M., Loretoni, R., Duranti, M., Ghavami, M., Dudley, S., & Tiberi, G. (2023). Radiation-Free Microwave Technology for Breast Lesion Detection Using Supervised Machine Learning Model. Tomography, 9(1), pp. 105-129.

[46] Conceição, R. C., Medeiros, H., O'Halloran, M., Rodriguez-Herrera, D., Flores-Tapia, D., & Pistorius, S. (2013). Initial classification of breast tumour phantoms using a UWB radar prototype. In 2013 International Conference on Electromagnetics in Advanced Applications (ICEAA), Turin, Italy, pp. 720-723.

[47] Henin, B., Abbosh, A. M., & Abdulla, W. A. (2015). Electro-biomechanical breast phantom for hybrid breast imaging. In 2015 International Symposium on Antennas and Propagation (ISAP), Hobart, TAS, Australia, pp. 1-3.

[48] Abu Bakar, A., Abbosh, A., & Bialkowski, M. (2011). Fabrication and characterization of a heterogeneous breast phantom for testing an ultrawideband microwave imaging system. In 2011 Asia-Pacific Microwave Conference Proceedings (APMC), 4 p.

[49] Lai, J., Soh, C., Gunawan, E., & Low, K. (2010). Homogeneous and heterogeneous breast phantoms for ultra-wide band microwave imaging application. Progress In Electromagnetics Research, 100, pp. 397-415.

[50] Islam, M. T., Samsuzzaman, M., Kibria, S., & Islam, M. T. (2018). Experimental Breast Phantoms for Estimation of Breast Tumor Using Microwave Imaging Systems. IEEE Access, 6, pp. 78587-78597.

[51] Oliveira, B., O'Loughlin, D., O'Halloran, M., Porter, E., Glavin, M., & Jones, E. (2018). Microwave Breast Imaging: Experimental tumour phantoms for the evaluation of new breast cancer diagnosis systems. Biomedical Physics & Engineering Express, 4 p.

[52] Monacelli, G., Canicattì, E., Monorchio, A., Vispa, A., Sani, L., & Tiberi, G. (2021). Electromagnetically characterized gelatinous-based phantoms for breast microwave imaging. In 2021 IEEE International Symposium on Antennas and Propagation and USNC-URSI Radio Science Meeting (APS/URSI), Singapore, pp. 357-358.

[53] Särestöniemi, M., Dessai, R., Myllymäki, S., & Myllylä, T. (2023). A Novel Durable Fat Tissue Phantom for Microwave Based Medical Monitoring Applications. In EAI BICT 2023 - 14th EAI Int. Conf. on Bio-inspired Information and Communications Technologies, April 2023.

[54] Särestöniemi, M., Sonkki, M., Myllymäki, S., & Pomalaza-Raez, C. (2021). Wearable Flexible Antenna for UWB On-Body and Implant Communications. Telecom, 2(3), pp. 285-301.

[55] Wang, Z., Qin, L., Chen, Q., Yang, W., & Qu, H. (2019). Flexible UWB antenna fabricated on polyimide substrate by surface modification and in situ self-metallization technique. Microelectronic Engineering, 206, pp. 12-16.

[56] Kokkonen, M., Dessai, R., & Myllymäki, S. (2023). Implementation of a second-order frequency selective surface filter at mmWave using paper and silver ink. Journal of Engineering, e12249.

[57] IT'IS Foundation. (2022). Dielectric Properties. Retrieved from https://www.itis.ethz.ch/virtual-population/tissue-properties/databaseM